UNIVERSITEIT VAN PRETORIA
UNIVERSITY OF PRETORIA
YUNIBESITHI YA PRETORIA

Clean coal technology using process integration: A focus on the IGCC

By

Vhutshilo Madzivhandila

A thesis submitted in fulfilment of the requirements of the degree

Master of Engineering (Chemical)

In the

Faculty of Engineering, Built Environment and Information Technology

University of Pretoria

Pretoria

December 2010

Supervisor: Prof. T Majozi

© University of Pretoria

Abstract

The integrated gasification combined cycle (IGCC) is the most environmentally friendly coal-fired power generation technology that offers near zero green house gas emissions. This technology has higher thermal efficiency compared to conventional coal-fired power generation plants and uses up to 50% less water.

This work involves the optimization of IGCC power plants by applying process integration techniques to maximize the use of energy available within the plant. The basis of this project was the theoretical investigations which showed that optimally designed and operated IGCC plants can achieve overall thermal efficiencies in the regions of 60%. None of the current operating IGCC plants approach this overall thermal efficiency, with the largest capacity plant attaining 47%. A common characteristic in most of these IGCC plants is that an appreciable amount of energy available within the system is lost to the environment through cold utility, and through plant irreversibility to a smaller extent.

This work focuses on the recovery of energy, that is traditionally lost as cold utility, through application of proven process integration techniques. The methodology developed comprises of two primary energy optimization techniques, i.e. pinch analysis and the contact economizer system. The idea behind using pinch analysis was to target for the maximum steam flowrate, which will in turn improve the power output of the steam turbine. An increase in the steam turbine power output should result in an increase in the overall thermal efficiency of the plant. The contact economizer system is responsible for the recovery of low potential heat from the gas

turbine exhaust *en route* to the stack to heat up the boiler feed water (BFW). It was proven in this work that a higher BFW enthalpy results in a higher overall efficiency of the plant.

A case study on the Elcogas plant illustrated that the developed method is capable of increasing the gross efficiency from 47% to 55%. This increase in efficiency, however, comes at an expense of increased heat exchange area required to exchange the extra heat that was not utilized in the preliminary design.

Dedication

To my mom, dad and Bernice with love

Declaration

UNIVERSITY OF PRETORIA
FACULTY OF ENGINEERING, BUILT ENVIRONMENT AND IFORMATION TECHNOLOGY
DEPARTMENT OF CHEMICAL ENGINEERING

The Department of CHEMICAL ENGINEERING places great emphasis upon integrity and ethical conduct in the preparation of all written work submitted for academic evaluation.

While academic staff teach you about systems of referring and how to avoid plagiarism, you too have a responsibility in this regard. If you are at any stage uncertain as to what is required, you should speak to your lecturer before any written work is submitted.

You are guilty of plagiarism if you copy something from a book, article or website without acknowledging the source and pass it off as your own. In effect you are stealing something that belongs to someone else. This is not only the case when you copy work word-by-word (verbatim), but also when you submit someone else's work in a slightly altered form (paraphrase) or use a line of argument without acknowledging it. You are not allowed to use another student's past written work. You are also not allowed to let anybody copy your work with the intention of passing if of as his/her work.

Students who commit plagiarism will lose all credits obtained in the plagarised work. The matter may also be referred to the Disciplinary Committee (Students) for a ruling. Plagiarism is regarded as a serious contravention of the University's rules and can lead to expulsion from the University.

The declaration which follows must be appended to all written work submitted while you are a student of the Department of CHEMICAL ENGINEERING. No written work will be accepted unless the declaration has been completed and attached.

I (full names): **Vhutshilo Andani Madzivhandila**
Student number: **25195532**
Topic of work : **Clean coal technology using process integration: A focus on IGCC**

Declaration

Declaration

1. I understand what plagiarism is and am aware of the University's policy in this regard.
2. I declare that the material handed in (e.g. essay, report, project, assignment, dissertation, thesis, computer programme, etc) is my own original work. Where other people's work has been used (either from a printed source, internet or any other source), this has been properly acknowledged and referenced in accordance with departmental requirements.
3. I have not used another student's past written work to hand in as my own.
4. I have not allowed, and will not allow, anyone to copy my work with the intention of passing it off as his or her own work.

Signature 

Acknowledgements

It is with immense gratitude that I convey acknowledgements to:

- My supervisor, Prof. T Majozi, whose supervision, support and encouragement from the preliminary stage to the concluding stage of my studies enabled me to develop an understanding of the subject.
- The SUSPSE group for the positive criticism and suggestions during the research progress meetings.
- The SANERI Energy hub at the University of Pretoria for funding this project.

Contents

Nomenclature

a_H - heat transfer area

a_M - mass transfer area

ASU - air separation unit

c_s - humid heat

G - mass flowrate of the gas

H_{BFW} - enthalpy of the boiler feed water

H_G - enthalpy of the gas

H_i - enthalpy at the gas-liquid interface

H_L - enthalpy of the liquid

h_L - heat transfer coefficient of the liquid-phase

H_{sl} - enthalpy of the saturated liquid in the boiler

H_{sps} - enthalpy of the superheated steam leaving the HRSG

H_{ss} - enthalpy of the saturated steam leaving the boiler

k_G - gas-phase mass transfer coefficient

L - mass flowrate of the liquid

T_i - temperature at liquid-gas interface

T_L - liquid phase temperature

T_0 - reference temperature

1 - top of the packed bed column

2 - bottom of the column

$\dot{m}$ - maximum boiler feed flowrate

W_{GT} - gas turbine power output

W_{ST} - steam turbine power output

Y - humidity of the gas

Z - tower height

Greek symbols

η_{ST} - thermal efficiency of the steam turbine

λ_0 - latent heat of vaporization of water at reference temperature T0

λ_V - latent heat of vaporization of water

1. INTRODUCTION

1.1 Background

Coal is a dominant source of fuel for power generation in most countries due to its abundance and low cost. Over the years, coal gained a negative reputation as an environmentally destructive energy resource due to the level of CO_2 emissions associated with it. The main sources of these emissions are coal fired power plants and coal to liquids technology. Recent work has, however, overturned this negative reputation by shifting the focus of power generation back to coal. Better coal technologies that are more environmentally friendly have been developed for power generation, but still require some improvements.

The integrated gasification combined cycle (IGCC) is one of the innovative electric power generation processes. This technology combines modern coal gasification with gas turbine and steam power generation. Gasification technology grew in the European oil refineries in the early 1950s mainly for the disposal of low value refinery by products (Profiles, 2006). These by products were gasified to produce H_2 and/or feedstock that were used in the manufacture of chemicals such as ammonia and fertilizers. Economic considerations, however, drove subsequent developments to focus on using coal as primary feedstock for gasification to produce the aforementioned H_2 and feedstock. A few years later, increasing stringent emissions legislation and the concerns over security of national energy supply in Europe led to

the integration of coal gasification with the combined cycle. This resulted in the construction of the first IGCC plant, the Nuon project in Buggenum - Netherlands.

There are currently five commercially operating IGCC plants worldwide. Two of these plants are located in the U.S, two in Europe and one in Japan. The IGCC technology has proved to be one of the cleanest available technologies for coal-based electric power generation. It offers high system efficiencies and very low pollution levels. For these and other technical reasons, there is a steady increase in the number of IGCC projects that are being implemented.

1.2 The integrated gasification combined cycle

The integrated gasification combined cycle (IGCC) is an integration of two primary technologies, gasification and the combined cycle (gas turbine and the steam turbine). The combination of these two technologies divides the IGCC into two paths or subsystems, the gas-path and the steam-path. Although these two primary processes (gasification and the combined cycle) are well understood individually, their integration is complex due to mutual influences of each process on the final design and performance of the integrated system. This mutual dependence makes the optimization process of the IGCC a complicated problem.

In general, the IGCC process involves thermally converting coal into a synthetic gas (syngas), which after cleanup, is utilized to generate electricity in a combined cycle process. A typical IGCC power plant is made up of five main sections or units as listed below:

- The air separation unit (ASU)
- The gasification unit
- The syngas cooling and cleanup section
- The heat recovery section
- The combined cycle

The process followed by IGCC plants can be broken down into the following steps:

(i) Coal is gasified in a gasifier in the presence of oxygen (from the ASU) and steam to produce syngas.

(ii) The raw syngas is cooled then sent to the cleaning section where solid particles and other pollutants are removed.

(iii) Electricity is then generated in a combined cycle that follows the following steps:

- A mixture of clean syngas and a diluent (nitrogen or steam) is combusted in the gas turbine combustor then used to drive the gas turbine which generates about 60% of the total electricity.
- Heat carried by the exhaust gas from the gas turbine is used in the heat recovery steam generator (HRSG) to superheat the steam from the syngas cooler.
- The superheated steam is then used to drive the steam turbine which generates the other 40% of the total electricity.

Figure 1.1 illustrates the process followed by IGCC plants. The gas-path components include the ASU, the gasifier, the gas cleanup section and the gas turbine. The steam path on the other hand includes the boiler, the HRSG and the steam turbine. These two paths are integrated by the boiler and the HRSG to form one system.

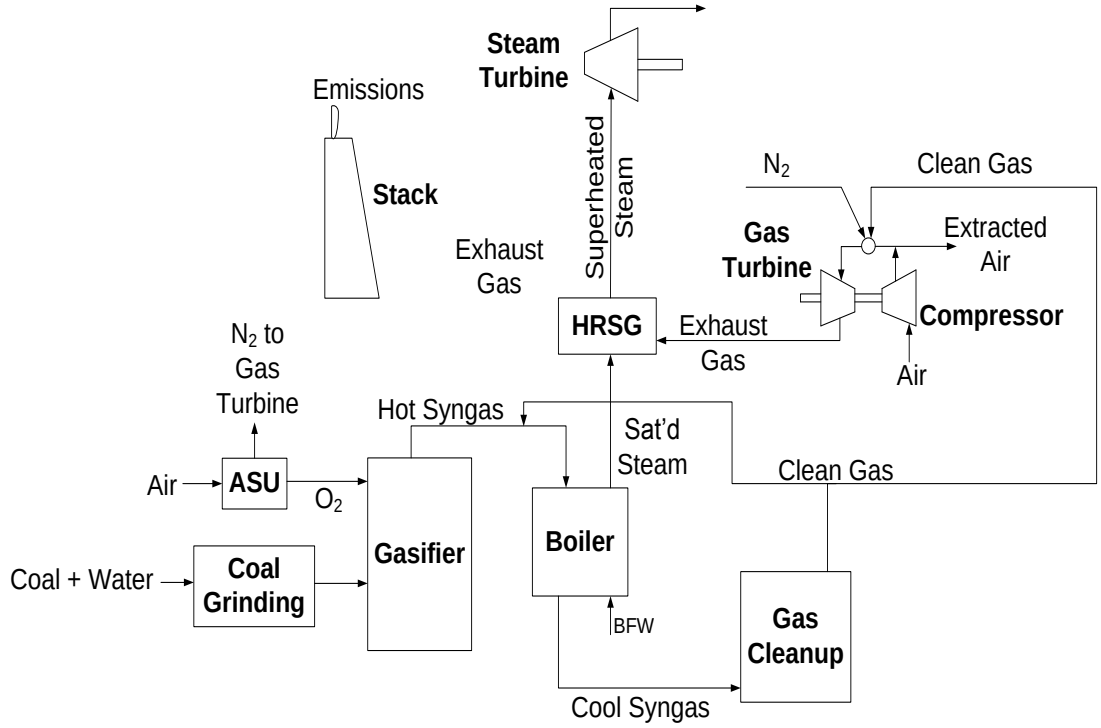

Figure 1.1: Simplified diagram of the IGCC process

Each component within the two paths has a vital role in the electricity generation process as discussed in the following paragraphs.

The air separation unit (ASU)

This section is made of the air compression system, air separation cold box, oxygen compression system and a nitrogen compression system. Atmospheric air is compressed by a multistage centrifugal compressor and cooled to about 5º C. The cooled air is then directed to the molecular sieve absorbers where moisture, CO_2 and contaminants are removed. This dry CO_2 free air is then filtered before separation into oxygen, nitrogen and waste gas in the air separation cold box. Cryogenic distillation is used to separate the dry filtered CO_2 free air into oxygen and nitrogen streams.

Oxygen produced by the ASU is about 95% pure. This oxygen is discharged from the cold box of the ASU and fed to the gasifier for use in the thermal conversion of coal to syngas. Oxygen from the ASU is also utilized by the sulfur recovery units. Nitrogen produced by the ASU is injected into the combustion zone of the gas turbine to increase mass flow in the combustion turbines and to reduce the formation of thermal NO_x. This Nitrogen is also used to blanket and purge inert systems.

The gasification unit

Three technology variants that are categorized by the gasifier configuration and according to their flow geometry exist (Minchener 2005):

- Entrained flow gasifiers
- Fluidized bed gasifiers
- Moving bed gasifiers

Most IGCC projects are focusing on entrained-flow slagging gasifiers (Zheng & Furinsky, 2005). In this section, coal is brought into contact with steam and oxygen or can simply enter as slurry. The function of the gasifier, which operates under high pressures and temperatures, is to thermally convert the coal to syngas. Oxygen (from the ASU) and the coal slurry fed to the pressurized gasifier to produce a syngas consisting primarily of hydrogen (H_2), carbon monoxide (CO) and carbon dioxide (CO_2) (US DoE, 2000). The syngas also contains noticeable amounts of hydrogen sulfide (H_2S), carbonyl sulfide (COS), fine particles, methane, argon, ammonia, nitrogen, and other compounds.

Ash that is present in the coal liquefies at gasifier temperatures and, when cooled, forms a by-product referred to as slag. The slag exits the gasifier separately from the syngas and is removed from the process by the slag handling system. This slag is less likely to cause environmental damage than fly ash from conventional coal plants (Shilling & Lee, 2003). Small amounts of fine particulate exit the gasifier with the raw syngas and are removed by the downstream cleanup systems. The raw syngas leaves the gasifier at temperatures in the regions of 1300ºC.

Boiler

The syngas exiting the gasifier must be cooled and cleaned prior to being used as a fuel in the gas turbine. This cooling process occurs in the syngas cooler where the syngas is cooled to lower temperatures in the regions of 300º C subsequent to quenching. The syngas cooler is a vertical shell and tube heat exchanger, with the hot

syngas in the tube side. This unit generates saturated high pressure steam. The saturated high pressure steam from this unit is superheated in the HRSG for use in the steam turbine generator.

Gas cleanup

The current gas clean up practice in IGCC systems is carried out by conventional absorption processes operating near ambient temperature (Giuffrida, Romano & Lozza, 2010). The first step in this gas cleaning process is scrubbing. This is done by a scrubber that utilizes water trays to wash and cool the syngas. The water scrubber removes the fine solids, as well as ammonia, chlorides, and other trace components that are water soluble. These components are removed to reduce the potential of corrosion within the piping and vessels, as well as reduce the formation of undesirable products in the acid gas removal (AGR) system. Solids removed by the scrubber are processed and either recycled with water to the coal slurry preparation system for re-injection into the gasifier or sent to the slag handling system.

Following the water scrubber, the syngas flows through a low temperature gas cooling system, which includes heat exchangers that improve heat rate and lower the syngas temperature to accommodate the operation of the AGR. The AGR system is designed to remove more than 99% of the total sulfur from the raw syngas. Primary sulfur compounds in the syngas are hydrogen sulfide (H_2S) and carbonyl sulfide (COS). Because COS is not readily captured by the AGR, a hydrolysis unit is utilized

upstream of the AGR to react the COS with water vapor in the presence of a catalyst to form H_2S and CO_2 as shown by reaction 1.

$$COS + H_2O \rightarrow H_2S + CO_2 \quad (1)$$

An activated carbon bed system is also included in the cleanup process and is expected to remove more than 90% of the mercury from the raw syngas. This mercury removal system is located downstream of the COS hydrolysis unit and upstream of the AGR system. Clean syngas exits the AGR system to a saturator that adds moisture to the syngas. The moisture from the saturator adds mass to the syngas to increase the gas turbine output and also lower combustion flame temperatures to reduce thermal NO_x formation.

The combined cycle power generation system

The gas turbine is the unit responsible for generating more power in the combined cycle. In this unit, the syngas discharged from the cleaning section is firstly mixed a diluent (Nitrogen) in the turbine combustor unit. The mixing of the syngas with a diluent has the following advantages:

- The increased flow through the gas turbine produces more power.
- The overall efficiency of the system is enhanced.
- The combustion temperature is lowered, resulting in reduced NO_x formation.

Air from the compressor of the gas turbine is used as an oxidant in the combustion chamber. The combustion process involves a lot of reactions to complete the oxidation process forming CO_2 and H_2O, the ultimate products of combustion. The combustion gases are fed into the gas turbine where the gas is expanded and electricity is generated. The exhaust gas from the gas turbine, which is still at high temperatures, is charged into the HRSG where saturated high pressure steam from the boiler is superheated. The superheated steam from the HRSG is used in the steam turbine to drive the turbine and generate electricity.

The IGCC process has proven to have several advantages over conventional coal power generation plants. A couple of these advantages are listed below (The Energy Blog, 2005):

- SO_x, NO_x, CO_2 and particulate emissions are much lower in IGCC plants than in conventional coal power plants.
- IGCC plants use 20-40% less water than conventional coal power plants.
- IGCC plants operate at higher efficiencies than conventional coal power plants, thus requiring less fuel and producing less emission. Thermal efficiencies as high as 47% have been achieved with efficiencies as high as 60% expected in the very near future using a high efficiency turbines and some other process improvements.

1.3 Basis and objectives of the study

This research was motivated by the observations made in practical IGCC systems after theoretical studies by various researchers. These theoretical studies have shown that even though IGCC plants are more efficient than conventional coal power plants, they are not operating at their full potential. A lot of studies have shown that the efficiency of the IGCC plants can be improved if certain sections of the plant are optimized. Operational experience of IGCC plants and the advanced technology currently developed have brought insight on ways to improve the system performance. The objective of this project was to optimize the use of energy within IGCC plants in order to improve the efficiency of the process. This work focuses on the steam-path of the system and no alterations were done on the gas-path of the system.

1.4 Thesis structure

This thesis is structured as follows:

- Chapter 1 introduces the IGCC and the purpose of this study
- Chapter 2 discusses the energy optimization tools relevant to this study and also reviews the work which has been done to optimize the performance of IGCC plants
- Chapter 3 focuses on the development of the methodology used to achieve the objective of this study.
- Chapter 4 discusses the application of the developed methodology
- Chapter 5 gives the conclusions and recommendations based on the study.

2. LITERATURE REVIEW

2.1 Introduction

This chapter discusses the energy optimization methods relevant to this study, i.e pinch analysis and the contact economizer system. Also included in this chapter is the review of the work previously done to improve the overall efficiency of IGCC plants. Several methods are discussed in detail and conclusions based on effectiveness/non-effectiveness of these methods are drawn.

2.2 Pinch Analysis

Pinch analysis is essentially a heat-flow based technique where system design problems are considered for identification of energy saving opportunities and modification of existing plants or for design of new energy efficient plants (Kemp, 2007). This technique has been broadly applied in the synthesis of heat exchanger networks and also mass exchanger networks and design. This section focuses on the application of pinch analysis to heat exchanger networks (HENs) only. The approach vests on concepts that are convenient and simple, and makes it possible to deal with problems considered complex. The technique puts emphasis on simple sums rather than complex mathematics.

The initial step in pinch analysis is performing heat and material balances of the process. This is succeeded by setting energy targets for saving energy prior to the design of the heat exchanger network.

Targeting for energy savings

The energy target set via pinch analysis is essentially for minimum energy consumption or maximum energy recovery. To set this target, process stream data is required. This leads us to the first and probably the most vital step of setting the energy target, i.e. data extraction. This step involves choosing streams that are necessary to carry out the analysis. This procedure is vital to ensure that there is no missed opportunity for heat recovery (Smith 2005).

In pinch analysis, a stream is defined as any flow that requires heating or cooling, but does not change in composition (Kemp, 2007). From this definition, hot streams and cold streams can be extracted from the process where the former are streams that require cooling and the latter being streams that require heating. Once the streams are extracted, essential data that includes the stream supply temperature (T_s), target temperature (T_t) and the duty (Q) is needed to continue with the targeting process. Prior to setting the energy targets, a minimum temperature difference (ΔT_{min}) is set. This ΔT_{min} is the minimum acceptable temperature approach between hot and cold streams at each end of the heat exchanger. Optimization procedures to obtain ΔT_{min} have been developed but certain ΔT_{min} values have been proposed in literature according to the type of flow and properties of the fluid (Kemp, 2007).

Two algorithmic approaches have been developed for pinch analysis to satisfy the cooling, heating, and power demands of a process. Composite curves and the "problem table" are the two popular algorithms with the "problem table" been the generally used algorithm. The composite curve algorithm combines a set of individual temperature vs. enthalpy curves to create two curves that give a visual profile of the availability of heating or cooling available from the process streams. This graphical technique requires a "graph and scissors" approach for sliding graphs relative to one another which might be imprecise and cumbersome for large scale problems. The "problem table" algorithm, first introduced by Linnhoff and Flower (1978), sets the energy targets algebraically. In this thesis, the focus is on the second method, i.e. the problem table algorithm, which is discussed in detail below.

The problem table algorithm involves setting up enthalpy balance intervals based on the supply and target temperatures of the hot and cold streams to allow for maximum possible heat exchange. These intervals are set in such a way that the hot streams and the cold streams are at least ΔT_{min} apart. This is done by employing shifted temperatures (T^*), which are set ½ ΔT_{min} above the cold stream temperatures and ½ ΔT_{min} below the hot streams temperatures. Two successive shifted temperatures make up an interval. Configuring the intervals in this way guarantees a possibility of full heat exchange within any interval. As a consequence, each interval will either have a net deficit or surplus heat as depicted by the enthalpy balance, but never both. Knowledge of the stream population within each interval simplifies the calculation of the enthalpy balance. Equation (2.1) is used to calculate the enthalpy balance for any

interval (i). ΔT^* in this equation represents the temperature difference between two successive shifted temperatures that make up any temperature interval (i).

$$\Delta H_i = (\Delta T^*)\left(\sum CP_H - \sum CP_C\right)_i \tag{2.1}$$

A key feature of these intervals is that any heat available in interval 'i' is hot enough to supply any duty in interval '$i+1$'. It is therefore possible to set up a heat "cascade", assuming at first that no heat is supplied to the hottest interval (1) from the hot utility. A heat cascade based on the aforementioned assumption would normally lead to negative enthalpies within some intervals of the cascade for non-threshold problems. This infeasibility can be overcome by supplying the hot utility with an amount of heat equal to the largest negative enthalpy within the cascade, then cascade this heat down the intervals. The net result of this operation is that the minimum utility requirements can be predicted and a special point called the "pinch point" can be located. This "pinch point" is defined as the point of closest approach between hot and cold streams. Its location within the feasible heat cascade is the point where the enthalpy flow is zero.

The important results from the "problem table" are the net heat flows at all shifted temperatures (T^*), which are used in the construction of the grand composite curve (GCC). A graph of the net heat flows against shifted temperatures is known as the GCC. The GCC represents the difference between the heat available from the hot streams and the heat required by the cold streams, relative to the pinch, at a given

shifted temperature (Kemp, 2007). Thus, the GCC is simply a graphical plot of the problem table. A typical GCC is shown in Figure 2.1.

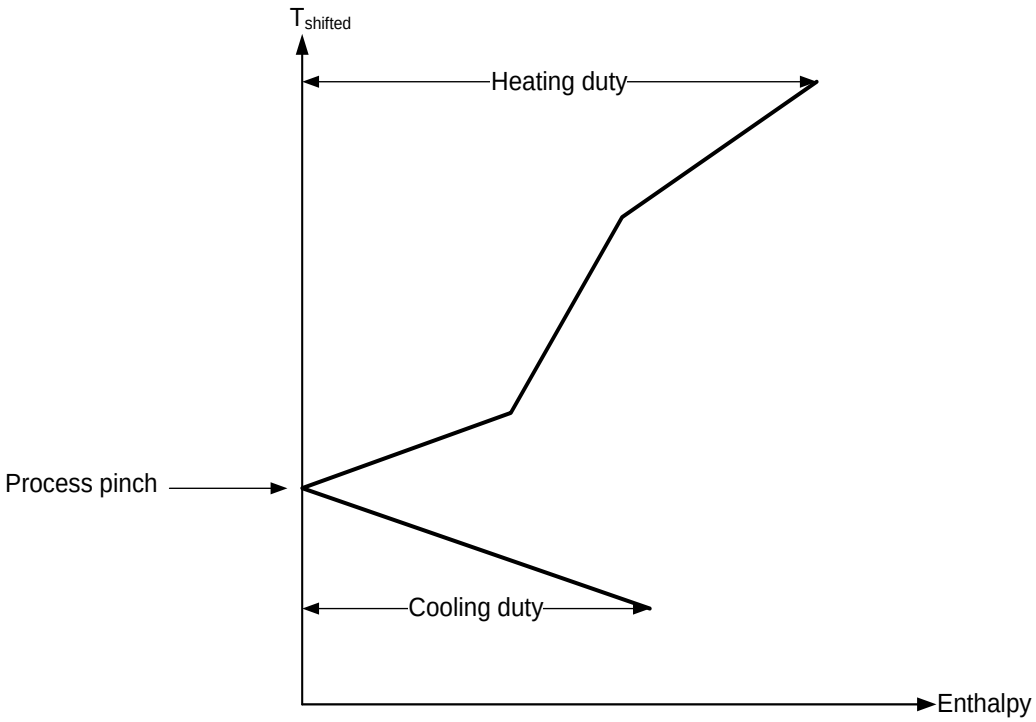

Figure 2.1: Typical representation of the grand composite curve

The GCC does not only show how much net heating and cooling is required, but also shows the temperature at which the net heating or cooling is needed. The pinch point can also be easily identified, being the point where the net heat flow is zero and the GCC touches the axis.

The GCC can also be used to target for multiple utilities where the general objective is to maximize the use of cheaper utility levels and minimize the use of expensive utility levels (Linnhoff, 1998), as shown in Figure 2.2.

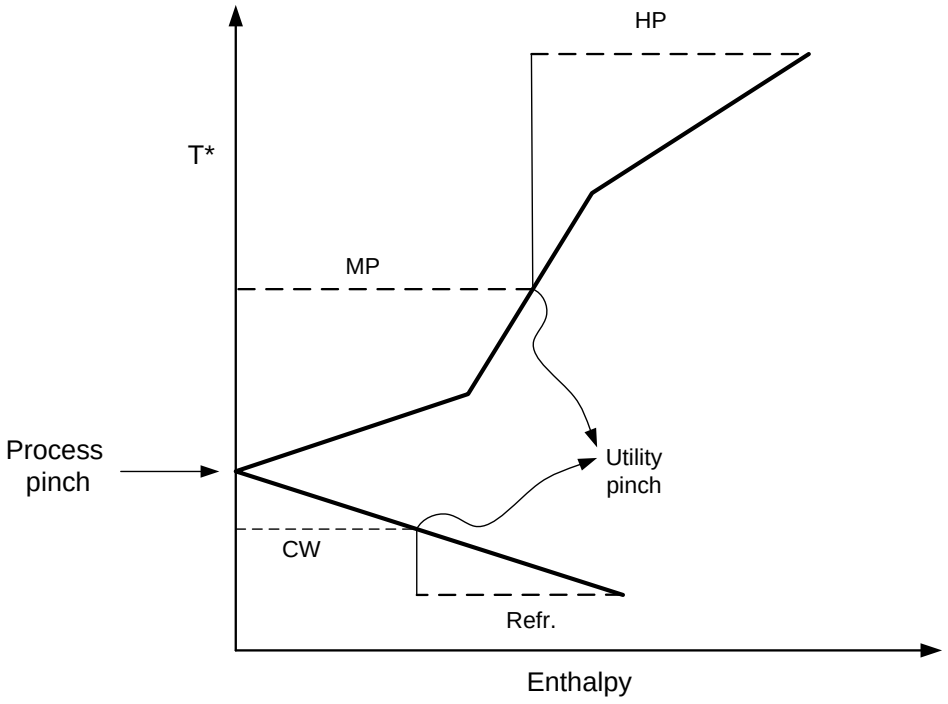

Figure 2.2: The grand composite curve for multiple utilities targeting

Designing for maximum energy recovery

The method used in designing for maximum energy recovery does not follow the traditional intuitive method for heat exchanger network design. In the traditional method, the engineer would normally start designing from the hot end then work his/her way towards the cold end. The downfall of this traditional method is that, despite the prior knowledge of the energy targets, it is difficult to design a network to achieve them (energy targets). The designer might have to go through a lengthy trial-and-error process to produce a heat exchanger network that might not even meet the energy targets. It is therefore imperative to use the insights given by pinch concepts to come up with design that meets the energy targets.

The pinch design method pursues the following three golden rules for maximum energy recovery or minimum energy requirement:

- Do not transfer heat across the pinch.
- Do not use cold utility above the pinch.
- Do not use hot utility below the pinch.

The critical aspect of this pinch design method is that it starts the design at the most constrained part of the problem, the pinch point. The thermodynamic constraints of the pinch are used to help the designer identify the critical hot and cold stream matches to produce efficient designs. A summary of this design method is as follows:

- Divide the problem at the pinch into two, i.e. one part above the pinch and the other below the pinch.
- Start the design on either side of the pinch (above or below), moving away from it.
- Immediately adjacent to the pinch, obey the following constraints while matching hot and cold streams:

  $CP_{HOT} \geq CP_{COLD}$ below the pinch for all cold streams

  $CP_{HOT} \leq CP_{COLD}$ above the pinch for all hot streams
- Maximize the exchanger heat loads for the corresponding stream matches.
- Supply the external cooling only below the pinch and the external heating only above the pinch.

A typical representation of a heat exchanger network is shown in Figure 2.3 where hot streams (H1 and H2) are matched with cold streams (C1 and C2). The pinch point, the line dividing the design into two as discussed earlier, is also indicated in Figure 2.3. External utilities are also shown in this Figure where the cold utility (C) is used for stream H2 and the hot utility (H) for stream C2.

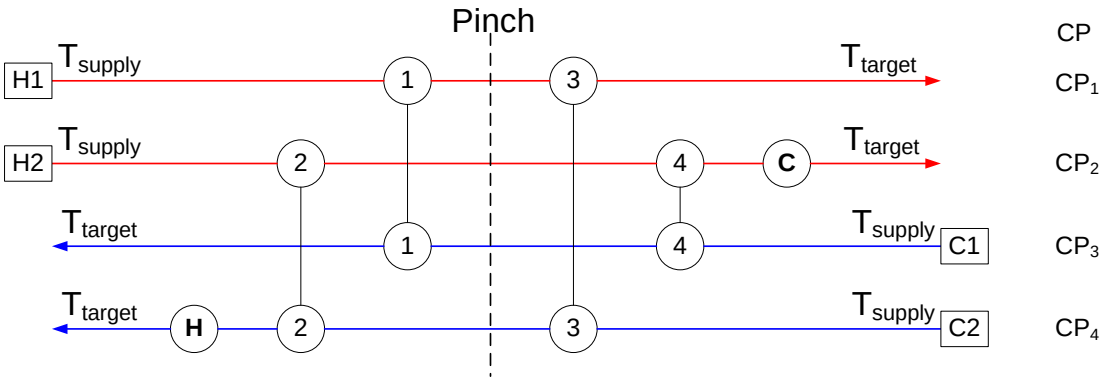

Figure 2.2.3: Basic representation of a heat exchanger network

2.3 The contact economizer system

The contact economizer system (CES) is a low potential heat recovery system allotted to explore the simultaneous management of heat and mass transfer between a gas stream and a liquid desiccant stream. Figure 2.4 represents a typical CES for the recovery of heat from a gas stream using water as a desiccant.

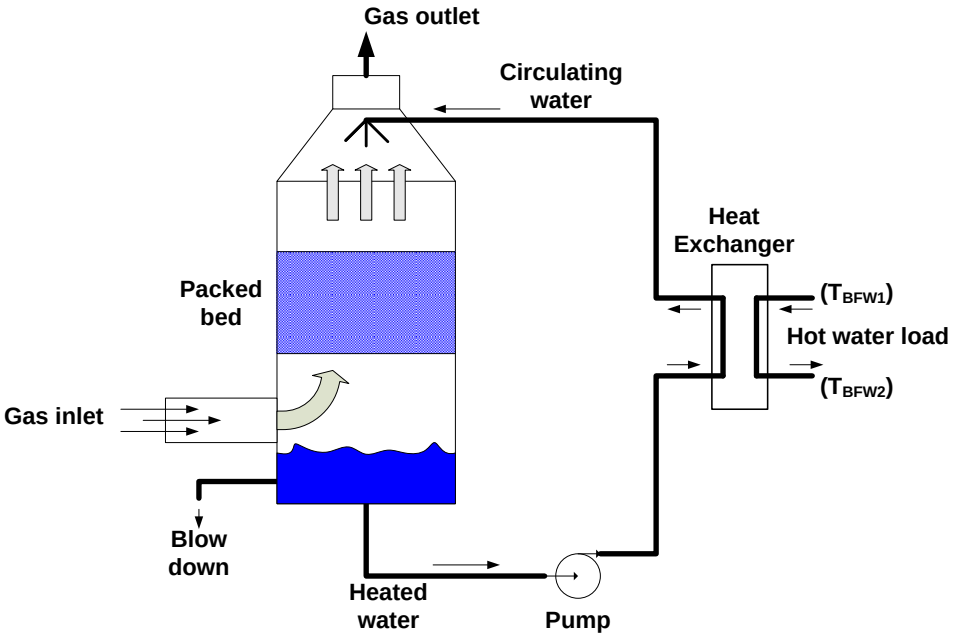

Figure 2.4: Basic structure of the contact economizer system

This process involves direct heat transfer between the hot gas stream and a cold circulating water stream accompanied by dehumidification of the gas, in a packed bed column. The heated desiccant that leaves at bottom of the packed bed column can then be used as a source of heat for other operations. Literature (Mickley, 1949) has shown that the circulating water can only be heated to a point where its temperature equals the wet-bulb temperature of the gas provided an infinite heat exchange area is available. At this point, fog formation is a possibility. Consequently, heat transfer within the column should be maintained in such a way that the circulating water leaves the column at a certain temperature "ΔT" degrees lower than the wet-bulb temperature of the gas at all times. This allows for thermal driving forces and also ascertains that fogging conditions will not be attained in the tower. "ΔT" values as low as 2.5°C are feasible for packed bed columns and have been previously demonstrated in literature (Zhelev & Semkov, 2004).

A brief derivation of the design equations for such dehumidification systems is given below, with a large portion of their development presented elsewhere (Venkataraman, 2009). Consider a differential height "dZ" of a forced draft, counter-current, adiabatic, constant cross-section dehumidification tower in which a gas and a liquid desiccant are directly contacted as shown in Figure 2.5.

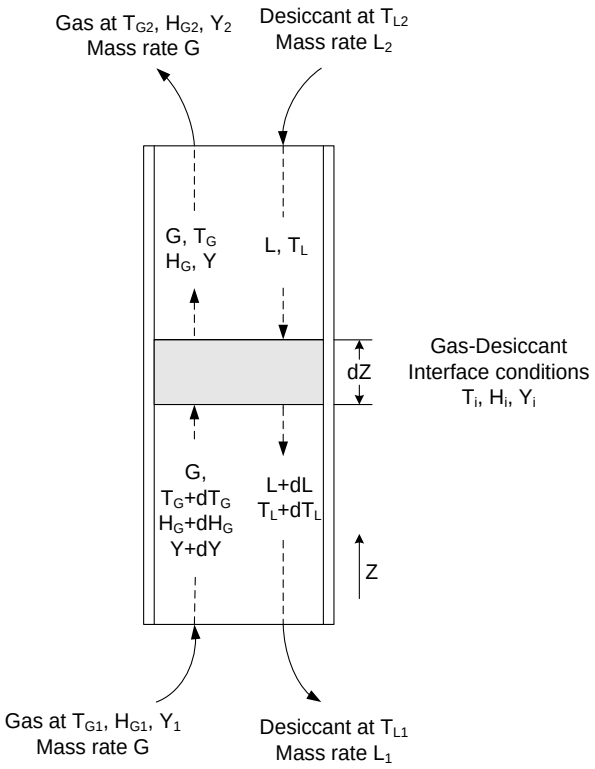

Figure 2.5: Schematic diagram of a forced draft dehumidification tower

The gas enters the differential section of the column at a mass rate of "G", a bulk temperature "$T_G + dT_G$", enthalpy "$H_G + dH_G$" and humidity "$Y + dY$". The liquid desiccant on the other hand enters the differential section at a mass rate "L" and a bulk temperature "T_L". In the differential section, the gas stream and the liquid stream exchange heat and mass then come out slightly changed. It is assumed that at the gas-

UNIVERSITEIT VAN PRETORIA
UNIVERSITY OF PRETORIA
YUNIBESITHI YA PRETORIA

liquid interface, the gas is saturated at the interface temperature "T_i". Heat transfer during such a dehumidification process can be viewed as a two path process; the first path being from the bulk gas-phase to the interface (will be referred to as the gas-path) and the second path from the interface to the bulk liquid-phase (will be referred to as the liquid-path). Division of the heat transfer into two separate paths is necessary due to the fact for the liquid-path, heat transfer is entirely a result of temperature potential whereas two mechanisms are involved in the gas-path heat transfer.

For the gas-path, heat is transferred as a result of both the temperature potential and the mass transfer (latent heat). The enthalpy of the humid gas is defined by Equation (2.2).

$$H_G = c_s(T_G - T_o) + \lambda_o Y \tag{2.2}$$

The expression for the change in the gas-path enthalpy in terms of temperature is given by Equation (2.3).

$$GdH_G = Gd[c_s(T_G - T_0) + \lambda_o Y] = Gc_s dT_G + G\lambda_o dY \tag{2.3}$$

The two terms on the far right hand side of Equation (2.3) represent sensible heat (temperature potential) transfer and the latent heat transfer respectively. These two terms can be further represented by Equation (2.4) and Equation (2.5) respectively.

$$Gc_s dT_G = -h_G a_H (T_G - T_i) dZ \tag{2.4}$$

$$G\lambda_o dY = -\lambda_o k_G a_M (Y_G - Y_i) dZ \tag{2.5}$$

For the liquid-path, Equation $(2.6a)$ is the expression for the change in enthalpy in terms of temperature.

$$Lcp_L dT_L = -h_L a_H (T_L - T_i) dZ \cong GdH_G \qquad (2.6a)$$

Upon integration, Equation $(2.6a)$ yields Equation $(2.6b)$, one of the basic equations used in determining the tower height as will be explained later.

$$\int_{H_{G1}}^{H_{G2}} \frac{dH_G}{(T_L - T_i)} = \frac{-h_L a_H Z}{G} \qquad (2.6b)$$

The design equations can now be derived by combining the equations above. A combination of Equation (2.3), Equation (2.4) and Equation (2.5) gives Equation (2.7), the basis of the first design equation.

$$GdH_G = -h_G a_H (T_G - T_i) dZ - \lambda_o k_G a_M (Y - Y_i) dZ \qquad (2.7)$$

The Lewis relation, given by Equation (2.8), can be introduced into Equation (2.7) assuming that the area for mass transfer (a_M) is equals to the area for heat transfer (a_H). Equation (2.8) has proved to be accurate for air-water systems. Substituting Equation (2.8) into Equation (2.7) leads to Equation (2.9).

$$\frac{h_G}{k_G} = c_s \qquad (2.8)$$

$$GdH_G = -k_G a_M [c_s (T_G - T_i) + \lambda_o (Y - Y_i)] dZ \qquad (2.9)$$

UNIVERSITEIT VAN PRETORIA
UNIVERSITY OF PRETORIA
YUNIBESITHI YA PRETORIA

Following the definition of a humid gas given by Equation (2.2), Equation (2.9) can be reduced to Equation (2.10).

$$GdH_G = -k_G a_M (H_G - H_i) dZ \tag{2.10}$$

Equation (2.10) can then be combined with Equation (2.6) resulting in our first design equation, the "tie-line", given by Equation (2.11). This tie-line represents the ratio of the relative rates of enthalpy transfer through the gas phase and the liquid desiccant phase.

$$\frac{H_G - H_i}{T_L - T_i} = -\frac{h_L a_H}{k_G a_M} \tag{2.11}$$

An enthalpy balance applied to the two combined phases yields Equation $(2.12a)$.

$$d(GH_G) = d[Lcp_L(T_L - T_o)] \tag{2.12a}$$

Normally, the change in the liquid rate due to condensation or evaporation would be negligible. This simplifies Equation $(2.12a)$ into Equation $(2.12b)$.

$$GdH_G = Lcp_L dT_L \tag{2.12b}$$

Upon integration, Equation $(2.12b)$ yields our second design equation,the "operating line", given by Equation $(2.12c)$. This operating line is a straight line connecting the gas enthalpy and the desiccant temperature.

$$(H_{G2} - H_{G1}) = \frac{Lcp_L}{G}(T_{L2} - T_{L1}) \qquad (2.12c)$$

A summary of assumptions under which these design equations operate is as follows:

- At the water-gas interface, the gas is saturated at the interface temperature T_i.
- The change in the water flowrate due to evaporation or condensation is negligible.
- The heat transfer area (a_H) is equal to the mass transfer area (a_M). This assumption holds if and only if the interfacial area of packing inside the tower is fully wetted.

A set back in the design of such dehumidification/humidification systems is the lack of information on the values of the mass transfer coefficient ($k_g a_M$) and heat transfer coefficient ($h_L a_H$). Published values of such coefficients are extremely insufficient to cover a range of design problems. Majority of the available rate coefficient data or correlations are in the form of over-all transfer coefficients. These over-all transfer data or correlations would be exact if the liquid-film heat-transfer coefficient is infinitely large or if the equilibrium curve is linear. These conditions are rarely met in practice and although the use of an over-all enthalpy coefficient to determine the

tower/column volume is usually satisfactory, application of an over-all driving force could lead to erroneous results. This is mainly the case to situations significantly different from the experimental conditions used to obtain the coefficients.

Mickley's graphical technique

Mickley (1949) presented a simple and improved graphical method for the design of forced draft air conditioning equipment. This method is an extension of the "enthalpy potential" method proposed by Merkel. Mickley's graphical method is still recognized as the most convenient method for determining the size of the equipment for direct contact systems. All operating conditions of the equipment can be quickly determined by this method, and the danger of fog formation ascertained.

Figure 2.6 represents typical results of Mickley's graphical technique applied to a dehumidification process to help explain the method. Curve 'EF' in this figure represents the equilibrium line or saturation curve constructed under the assumption that the gas at liquid-gas interface is saturated. $\overline{AB}$ is the operating line constructed from Equation $(2.12c)$ with point 'A' corresponding to the entering bulk-gas enthalpy and the leaving bulk-water temperature. The slope of this line is Lcp_L/G as indicated in Equation (2.4). The construction of the dehumidification path begins at point 'C', which represents the gas-water vapour mixture at the bottom of the tower. A tie line with slope $-h_L a_H/k_G a_M$ is drawn from point 'A' to intersect the equilibrium line at point 'G'. The coordinates of this intersection point are (T_i, H_i). Equation $(2.13a)$ is an equal counterpart of Equation (2.4) obtained by substituting Equation (2.8) into

the latter equation. The ratio of Equation (2.10) to Equation $(2.13a)$ is the basis of Mickley's graphical technique. This ratio is given by Equation (2.14). Integration of Equation $(2.13a)$ yields Equation $(2.13b)$, the second basic equation used in the calculation of the tower height.

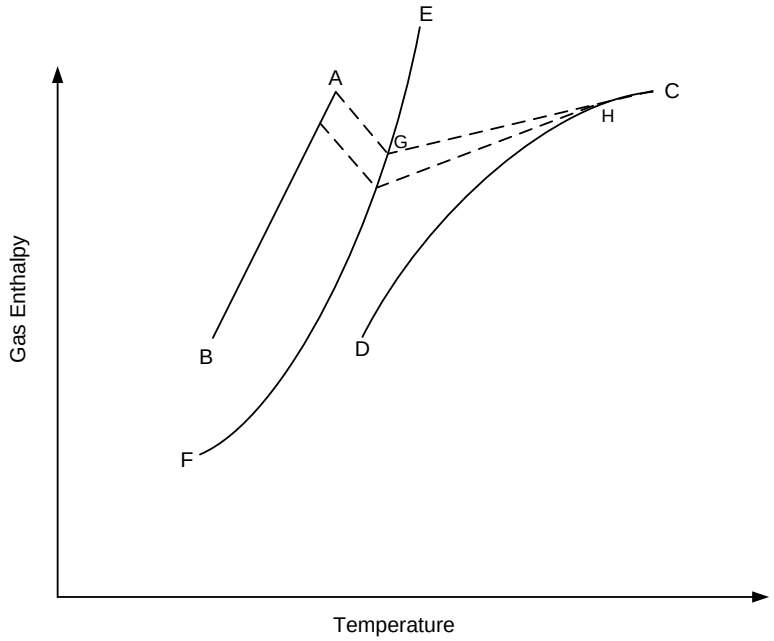

Figure 2.6: Enthalpy-Temperature diagram indicating the dehumidification process

$$G dT_G = -k_G a_H (T_G - T_i) dZ \qquad (2.13a)$$

$$\int_{H_{G1}}^{H_{G2}} \frac{dH_G}{(T_G - T_i)} = \frac{-k_G a_H Z}{G} \qquad (2.13b)$$

$$\frac{dH_G}{dT_G} = \frac{H_G - H_i}{T_G - T_i} \qquad (2.14)$$

A straight line drawn from point 'C' to point 'G' then gives the direction of the initial tangent to the gas path. The slope of this line is $(H_G - H_i)/(T_G - T_i)$, the ratio of the enthalpy driving force to the temperature driving force. By virtue of Equation (2.14),

the slope of $\overline{CG}$ also represents dH_G/dT_G, the rate of change of bulk-gas enthalpy with bulk-gas temperature. Assuming that this slope is constant over a small interval, point 'H' represents the bulk-gas enthalpy and temperature at a short distance above the bottom of the tower. The construction is extended with a new tie line and a new direction of the path line tangential to point 'H'. This exercise is repeated until a complete gas path ($\overline{CD}$) is achieved.

2.4 Methods for optimizing the IGCC

A lot of research on optimizing the efficiency or performance of the IGCC system is currently underway. This research can be categorized into the gas path optimization and integration, steam-path optimization and energy optimization. This section covers the work that has been successful in improving the overall performance of the IGCC.

Optimizing the gas-path of the IGCC has been the conventional way of optimizing the IGCC system. This type of optimization involves optimizing the performance of the gas-path components, i.e. the ASU, the gasifier, the gas cleaning unit and the gas turbine, and their integration. The integration of the IGCC components plays an important role in the overall performance of the system. One of the major integrations in the IGCC, depending on the design, exists between the ASU and the gas turbine. The ASU can either get its air supply from the gas turbine compressor or from an auxiliary compressor. These two situations represent an integrated system and a non-integrated system, respectively. Partial integration is also a possibility where a portion

of the air is supplied by the gas turbine and the remaining portion supplied by an auxiliary compressor.

A second interaction between the ASU and the gas turbine can be decided upon by the way the nitrogen from the ASU is treated. This nitrogen can either be supplied to the gas turbine as a diluent to reduce NO_x formation or it can be used elsewhere. This dilution also affects the operation of the gas turbine and the overall plant performance. The level of integration and the nitrogen supply ratio are, therefore, imperative in the optimization of the gas turbine performance. Most gas turbines are designed and optimized for the combustion of natural gas (Kim, Lee, Kim, Sohn & Joo, 2009). Since natural gas has a considerably higher heating value than syngas, there is more air compressor capacity than needed when using syngas as feed. For IGCC plants, this could turn out advantageous since some of the air extracted by the gas turbine could be supplied to the ASU while maintaining the same gas turbine power output. Increasing mass flow of the fuel (syngas) on the other hand can boost the power output of the gas turbine to the limits of the gas turbine expander flow, combustion temperature and expander blade material (Geosits & Lee, 2005).

Lee *et al.* (2010) did an analysis on the influence of the degree of integration between the ASU and the gas turbine on the performance of the gas turbine and the overall plant. Also included in this study was the influence of the ASU nitrogen supply ratio on the performance of the gas turbine and the overall plant. They defined the nitrogen supply ratio and degree of integration between the ASU and the gas turbine as shown by Equation (2.15) and Equation (2.16) respectively.

$$Nitrogen\ supply\ ratio = \frac{N_2\ supplied\ to\ GT\ combustor}{N_2\ separated\ from\ ASU} \tag{2.15}$$

$$Integration\ degree = \frac{Air\ to\ ASU\ from\ GT}{Total\ air\ to\ ASU} \tag{2.16}$$

The initial step in this study was to analyse the effect of the integration degree at a nitrogen supply ratio of 0%. The major operating parameters of the gas turbine were the surge margin, defined by Equation (2.17), and the combustion temperature. *PR* in Equation (2.17) represents the operating pressure ratio $\left(\frac{Pressure\ out}{Pressure\ in}\right)$ of the gas turbine while PR_{surge} represents the surge pressure ratio of the gas turbine.

$$surge\ margin = \frac{PR_{surge} - PR}{PR} \tag{2.17}$$

A common operating strategy in gas turbines is not to allow these two parameters to exceed the nominal or design values. In an IGCC plant design, *PR* may vary for a fixed combustion temperature depending on the integration degree. For a fixed *PR*, however, one would expect the combustion temperature to remain fixed but the opposite is the case since the combustion temperature could change. For this study, Lee *et al*. (2010) fixed the combustion temperature and examined the variation in *PR* with the integration degree. This study showed that the gas turbine power output increases with a decrease in the integration degree. This is the case because at low integration degrees, say 0%, the gas turbine requires a higher syngas mass flowrate, since no air is supplied to the ASU. The increase in the gas turbine power output with the decrease in the integration degree, on the contrary, results in a decrease in the

plant's overall efficiency. This can be attributed to the increase in auxiliary power required to compress the air required by the ASU with the decrease in the integration degree. The auxiliary power required to compress air required by the ASU amounts to about 25% of the air required by the gas turbine compressor at 0% integration degree. Another major downfall of operating at low integration degrees is decrease in the surge margin. An increase in the gas turbine inlet mass flowrate with decrease in the integration degree results in an increase in *PR* which inturn, reduces the surge margin. To sum up the facts, the overall plant efficiency increases with an increase in the integration degree despite the decrease in gas turbine power output. This increase in efficiency is, however, not that significant.

These results lead one to the second step of the study, i.e. the influence of the nitrogen supply ratio on the performance of the gas turbine and the overall plant. An increase in the nitrogen supply ratio results in an increase in the gas turbine power output. This is expected since the gas turbine inlet mass flow increases. The increase in the gas turbine power output in this case dominates the increase in auxiliary power required to compress the nitrogen, unlike in the previous case were air had to be compressed. Combining these results with the results obtained in the first step, i.e. examining the influence of the nitrogen supply at higher integration degrees, it was noted that both the gas turbine power output and the overall efficiency of the plant increase. Even with increase in the gas turbine inlet mass flowrate, *PR* did not increase as much as it increased at lower integration degrees where significantly higher inlet flowrates were the case. As a matter of fact, at 100% integration degree and 100% nitrogen supply, the surge margin was slightly lower than the design surge margin, which is

UNIVERSITEIT VAN PRETORIA
UNIVERSITY OF PRETORIA
YUNIBESITHI YA PRETORIA

acceptable. At lower integration degrees, however, the surge margin decreased drastically with an increase in nitrogen supply. Therefore, if a gas turbine is adopted in an IGCC system without any modifications, it is imperative to operate at high integration degrees and nitrogen supply ratios for better performance of the gas turbine and the overall plant.

Vlaswinkel (1992) presented methods to analyse and optimize the energetic performance of an IGCC plant as a whole. His methods involved the application of an exergy analysis which indicates the plant irreversibility in a multi-component plant and how irreversibility is distributed among the components of the plant. Also included in the methodology was pinch analysis that was developed by Linnhoff and Flower (1978), which provides a platform for optimum integration of the plant components to achieve a total energy optimization. The exergy analysis on the main units of the plant pinpoints the areas that contribute to the useful energy loss. It also signifies the quantity of energy loss due to plant irreversibility. This analysis gives the designer a platform to optimize or improve the use of energy in the pinpointed units.

Due to the mutual dependence of the plant units and the effect of their dependence on the overall performance of the plant, Vlaswinkels (1992) applied exergy analysis and pinch analysis in an iterative manner to optimize the plant as a whole. This iterative procedure is given in Figure 2.7. Construction of the grand composite curve (GCC) allows the designer to analyse certain areas of the plant where improvements can be made, correlate the results with those from the exergy analysis then optimize the plant.

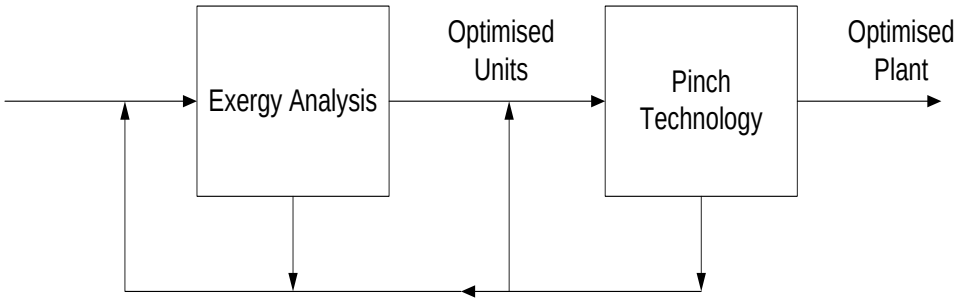

Figure 2.7: Iterative application of the design methodology by Vlaswinkels (1992)

This iterative procedure is based on the designer's intuition and makes it difficult for different designers to come up with the same optimum plant. The advantage of this method is that the exergy analysis shows the amount of usable energy loss through the units of the plant unlike an energy analysis that gives the total energy loss including the irreversible energy. Possible improvements to recover the usable energy, which in-turn improves the overall thermal efficiency of the plant, can be made. The disadvantage of this method, however, is that it does not give a clear indication of what needs to be done to improve the process and in most cases improving certain sections of the plant has a negative influence on the overall performance of the plant due to the mutual dependence of the plant's sections.

An interesting approach to the optimization of IGCC plants was recently developed by Emun *et al.* (2010). Their approach involved process optimization by sensitivity analysis and heat integration subsequent to simulating the IGCC process in Aspen Plus ® linked with Excel ™. The sensitivity analysis for different operating conditions is the first optimization step in this approach where only variables with a high impact on the performance indicators were selected. The performance indicators

were divided into two categories, i.e. economic and environmental. Carbon conversion efficiency, cold gas efficiency and thermal efficiency fell under the economic indicator category, while emission levels of NO_x, SO_2 and CO_2 per unit of net power output fell under the environmental indicator. The variables considered for optimization in this case were the gasification temperature, the gas turbine inlet temperature, the level of N_2 injection and the solids concentration in the coal slurry. These variables were individually optimized by analysing their effect on the performance indicators.

The second optimization step in this approach was analysing the effect of heat integration between the gasifier and the gas turbine combustor on the thermal efficiency and environmental performance. In this analysis, the authors basically wanted to take advantage of the endothermic nature of gasification and the exothermic nature of combustion in the gas turbine combustor. The idea was to supply the gasifier with heat from the gas turbine combustor and analyse the effect of varying the oxygen and the air requirements of the two units, respectively, on the thermal efficiency and the environmental performance. This analysis was supplemented by the heat integration of the ASU and the cleaning unit. Due to availability of high quality heat from the amine regenerator unit, the oxygen stream from the ASU to the gasifier was heat integrated with the condenser of the amine regenerator. Pinch analysis was later applied to the process to evaluate the overall process utility consumption and further potential for heat integration and energy production. Thermal efficiencies as high as 45% with the corresponding CO_2 and SO_x of 698 kg/MWh and 0.15 kg/MWh,

UNIVERSITEIT VAN PRETORIA
UNIVERSITY OF PRETORIA
YUNIBESITHI YA PRETORIA

respectively, based on an IGCC process model developed for a Texaco gasifier, can be attained with this approach.

The optimization of the steam-side subsystem is attracting more attention with the development of technology and the experience achieved. The majority of optimization methods for the steam-path involve simulation and analysis of the performance of the IGCC under the conditions of a given steam-path configuration. These conventional methods analyse the system performance numerically under the conditions of the given configuration in which parameters are optimized individually. The relevant processes in this case are mostly dependent on the designer's experience. The interdependence of variables is hardly considered in these conventional methods. This type of optimization method usually results in partial optimization due to the mutual dependence between the configuration and parameters of the steam-path.

Jiang *et al.* (2002) presented a method to overcome the shortcomings of the previously attempted methods on the steam-path. The model developed is based on a modular modelling idea of general system integration. This optimization method involves the construction of a super-structure for the steam-path which includes various kinds of feasible configurations. The parameters of the super-structure are then thermodynamically optimized to finally obtain an optimal steam subsystem. In short, the essence of this method is turning configuration optimization into parameter optimization of a super-structure to develop an optimized model for the steam-path. Their method was intended to adapt to various IGCC technological demands for the

steam subsystem and also to realize better cascade utilization of the exhaust heat from the gas turbine.

Syngas cleanup is one of the most important factors in IGCC plants that play a role in the overall performance of the system. The main characteristic of the syngas cleaning process is how the removal of sulfur containing components, mainly H_2S, is handled. In the current designs of the IGCC, gas cleanup is carried out by conventional absorption processes operating at near-ambient temperatures. In this type of cleaning process, the syngas is cooled to temperatures in the regions of 35°C before the removal of H_2S. The cooling process is necessary due to the fact that the absorbents used, usually methyldiethanolamine (MDEA), perform better at lower temperatures. This cooling process has been criticised for lowering the energy quality of the syngas stream. This led to a study of better ways to treat the syngas without compromising its energy quality or doing so to a smaller extent.

Syngas treatment at higher temperatures has been intensively studied in the past decade. The main difference between this type of treatment and cold syngas treatment is the desulfurization temperature. The desulfurization temperature of cold syngas treatment is near-ambient as explained above while the desulfurization temperature in hot syngas treatment can be as high as 650°C. The desulfurization process for hot gas cleanup is relatively simple compared to the cold syngas cleanup process. This process, as summarized in the review by Vamvuka *et al.* (2004), is made up of two primary units, i.e. a fluidized bed reactor attached to a cyclone and a sorbent regenerator attached to a different cyclone. Hot syngas enters the fluidized bed reactor

where it fluidizes the sorbent and thus react with it. The sorbents used for this process are normally metal oxides (ZnO) which react with the H_2S in the syngas to form a solid metal sulfide (ZnS). The sulfur-laden solids are collected by the cyclone and ducted to the regeneration reactor where they are reacted with oxygen to regenerate the metal oxide. The syngas from the top of the cyclone is passed through hot gas filters where it is cleaned of fines before removal of other contaminants (HCl, NH_3, HCN etc). A detailed discussion of the removal of other contaminants, which have a negligible impact on the performance of the plant, is given in a study by Ohtsuka *et al.* (2009).

Very few studies in the field of hot syngas cleanup have considered the effect of cleaning syngas at higher temperatures on the overall performance of the plant. Giuffrida *et al.* (2010) recently did a thermodynamic assessment of hot syngas cleanup on the performance of IGCC power plants. In this study, two base case simulations that employ cold gas cleanup and hot gas cleanup, with emphasis on their effect on the turbine power outputs and the thermal efficiency of the plant, were compared. For the hot gas cleanup simulation, the desulfurization temperature was initially set at 550°C then later altered to determine its effect on the thermal efficiency of the plant. This study showed that the thermal efficiency of an IGCC design with hot syngas cleanup can reach up to 2.4% more efficiency than an IGCC design with cold syngas cleanup. This higher efficiency can be attributed to the smaller auxiliary power required to compress nitrogen for dilution in the combustor, since part of the nitrogen from the ASU is used in the sorbent regeneration process and only a small

UNIVERSITEIT VAN PRETORIA
UNIVERSITY OF PRETORIA
YUNIBESITHI YA PRETORIA

portion is required for dilution. The turbine power outputs (gas turbine and steam turbine) were, however, slightly lower in the simulation with hot syngas cleanup.

The lower steam turbine power output of the simulation with hot syngas cleanup can be attributed to the lower energy recovery in the syngas coolers, since the cleaning process occurs at higher temperatures. The lower gas turbine power output on the other hand can be attributed to the lower gas turbine inlet flowrate, since part of the nitrogen produced in the ASU is used in the sorbent regeneration process to control the oxygen level. The effect of the desulfurization temperature on thermal efficiency of the plant was found to be negligible in the temperature range of 400°C-650°C. However, the desulfurization temperature has an effect on the NO_x emissions as would be expected. This effect can be avoided by considering syngas dilution by steam just like in cold syngas cleanup.

Carbon dioxide (CO_2) capturing is another field of interest in clean coal technology, especially in IGCC plants. Numerous methods to capture CO_2 are available and can be classified under pre-combustion, post-combustion and oxy-combustion of the syngas. Pre-combustion CO_2 capturing, as the name suggests, involves capturing the CO_2 present in the syngas before combustion in the gas turbine. In this process, CO in the syngas is reacted with steam in a gas shift reactor to produce a gas mixture mainly composed of CO_2 and H_2. The CO_2 is then separated from the gas mixture and the remaining gas, mainly composed of H_2, is sent to the gas turbine for combustion. In the post-combustion process, a solvent is used to capture CO_2 after combustion as the name suggests. The solvent is then regenerated for reuse in the capturing process and

the recovered CO_2 is transported for storage underground. The oxy-combustion CO_2 capturing process is the same as the post-combustion CO_2 capturing process except that pure oxygen is used for combustion in the gas turbine.

The IEA (2007) did a study on the effect of carbon capturing on the efficiency of IGCC plants and other power plants which are not relevant for this study (natural gas combined cycles and pulverised fuel combustion steam cycles). In this study, they compared the efficiency of IGCC plants with CO_2 capturing with the efficiency of IGCC plants without CO_2 capturing. Pre-combustion CO_2 capturing was used in this study as it was suggested to be the best suited process for IGCC plants (Lou, Smith & Sadhukhan, 2008). This study showed that IGCC plants with CO_2 capturing have a lower thermal efficiency than IGCC plants without CO_2 capturing. This can be attributed to the auxiliary power needed for CO_2 capturing and the reduction in the inlet mass flowrate to the gas turbine compressor. The lower efficiency, including the high capital cost of including carbon capturing in IGCC plants has hindered application of this process in industry.

The exergy-recuperative IGCC system is also one of the fields of interest in clean coal technology. In the conventional IGCC design, gasification is a highly endothermic reaction that acquires heat from the combustion of coal. The combustion of coal, however, results in large exergy losses due to the transformation of chemical energy into thermal energy (Kuchonthara, Battacharya & Tsutsumi, 2005). It is therefore imperative to use a gasification process that will minimize the exergy loss. The exergy-recuperative IGCC system employs steam gasification. The difference

between steam gasification and conventional gasification is the ratio between steam and oxygen. Steam gasification has a higher steam ratio than conventional gasification and produces syngas with higher hydrogen content, which results in higher cold gas efficiencies. The exergy recuperation in the aforementioned process occurs at the gas turbine where a portion of the gas turbine exhaust is used to generate steam for gasification. The other portion of the gas turbine exhaust is used in the HRSG, just like in the conventional IGCC design. This process reduces the auxiliary power required in the ASU for production and supply of oxygen due to the higher steam to oxygen ratio. The exergy recuperative IGCC system, along with improved gasification processes discussed below, is expected to increase the gross efficiency by up to 10% as compared to conventional IGCC designs.

The gasification unit (gasifier) is the main unit in IGCC plants that influences the overall performance of the system. In the current design of the IGCC, entrained flow gasifiers are used with either dry coal feed or coal slurry feed. Three main processes occur in the gasifier in the following order; pyrolysis, combustion and gasification. Pyrolysis is responsible for releasing volatiles and produce char particles while the combustion process is responsible for supplying the necessary heat for gasification. Gasification in such cases is influenced by a number of factors. When these three processes occur in the same unit, the produced tar, inorganic gases and the light hydrocarbon gases could severely hinder the gasification of char (Bayarsaikhan, Sonoyama, Hosokai, Shimada, Hayashi & Li, 2006). This interaction amongst these processes has recently triggered a study that was proposed over 30 years ago, i.e. the dual-bed circulating fluidized bed system (DBCFB).

In the DBCFB system, coal can be pyrolysed and gasified in one bed and the remaining unreacted char combusted in another bed. The heat of combustion is transported from one bed to the other through circulation of inert material such as sand between the two beds. This system was recently incorporated in high-efficiency steam gasification processes for the production of syngas as shown in Figure 2.8 (Bi & Liu, 2010; Corella *et al.*, 2007; Hayashi *et al.*, 2006). In this process, steam is used in the initial bed to pyrolyse and gasify coal. The unreacted char, along with the inert circulating material, is then sent to the second bed where oxygen is used for combustion. The hot inert material is then re-circulated back to the initial bed to initiate the pyrolysis. This steam gasification process results in higher cold gas efficiencies than conventional gasification processes.

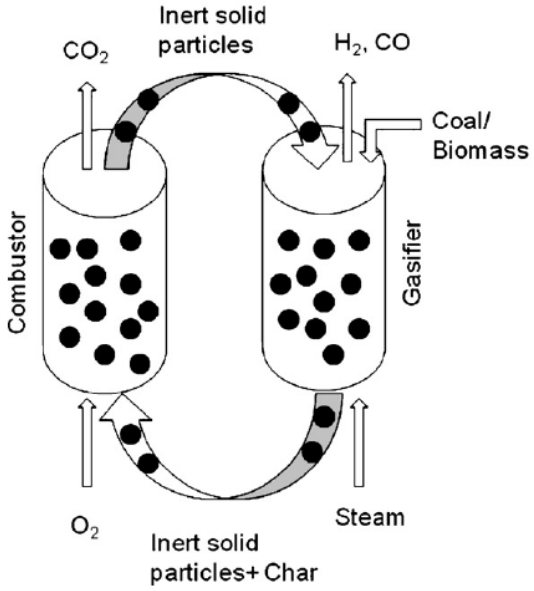

Figure 2.8: Dual-bed circulating fluidized bed gasification system

Gaun *et al.* (2010) recently combined this circulating fluidized bed technique with the exergy-recuperative IGCC system, with a few modifications included. Instead of using a DBCFB system, Guan *et al.* (2010) proposed a triple-bed circulating fluidized bed (TBCFB) system. This system, as the name suggests, is made up of three beds as shown in Figure 2.9.

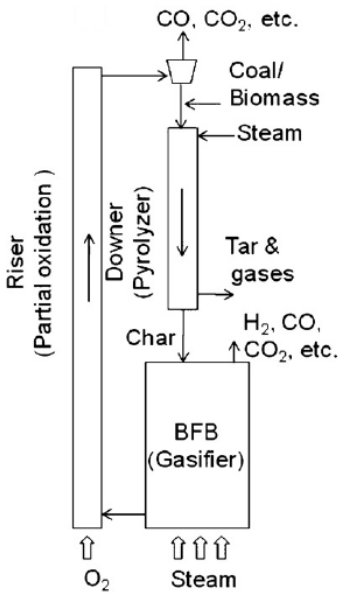

Figure 2.9: Triple-bed circulating fluidized bed gasification system

The first bed is the pyrolyzer (referred to as the downer) responsible the pyrolysis of coal. The second bed is the bubbling fluidized bed (BFB) gasifier responsible for the gasification of char. The final bed is the combustor (referred to as the riser) responsible for combustion of the unreacted char.

The process starts at the downer where a portion of the steam generated through exergy-recuperation at the gas turbine is fed to pyrolyse the coal for the production of

char. Tar and gases, the bi-products of pyrolysis, are separated from the char using a gas-solid separator. The resulting char is sent to the BFB gasifier, which operates at temperatures in the range of 700-900°C, where steam gasification takes place to produce syngas. The unreacted char, along with the circulating inert material, is sent to the riser for combustion with oxygen. The hot inert material is then re-circulated back to the downer to initiate pyrolysis. Calculations showed that this advanced IGCC system can reach gross efficiencies as high as 59%. Application of this system, however, is still hindered by certain challenges such as maintaining high density and solids flux necessary in the pyrolyzer, the development of non-mechanical gas seals suitable for the high density solids flow, etc. Research to overcome such challenges is currently underway.

2.5 Conclusion

Different methods to improve the efficiency of IGCC systems were reviewed in the preceding section. These methods can be divided into three categories, i.e. gas-path optimization where the components of the gas-path are optimized and integrated, steam-path optimization and energy optimization. It is evident form the review that a lot of studies focus on the gas-path optimization, with very few studies focusing on steam-path and energy optimization. The optimization methods presented, except for the CO_2 capturing method, are capable of achieving an increase in the overall efficiency of the IGCC system. Most of these methods presented achieve the increase in the overall efficiency by lowering the auxiliary power needed in the IGCC system. Only a few of these presented methods achieve the increase in the overall efficiency

by increasing the turbine power outputs. A common shortcoming of these methods, including the energy optimization methods, is that they do not maximize the use of energy available within the system. In most of the cases presented, if not all, a considerable amount of energy is lost to the environment as cold utility since IGCC plants require net cooling. It is therefore imperative to develop methods that will maximize the use of energy within IGCC system and improve the overall efficiency.

3. METHODOLOGY DEVELOPMENT

3.1 Introduction

This chapter deals with the development of the methodology used to optimize the use of energy within IGCC power plants. The methodology is divided into 2 parts, i.e. pinch analysis and the contact economizer system, and their development will be discussed separately. IGCC power plants can be viewed as combination of two subsystems, i.e. the gas-path subsystem and steam-path subsystem, as discussed extensively in section 1.2 of Chapter 1. The first part of the methodology, i.e. pinch analysis, focuses on the steam-path subsystem. The main reason of using pinch analysis was to maximize the use of energy within the IGCC system in order to increase the overall efficiency of the system. Section 3.2 discusses how the task of maximizing the use of energy via the steam-path subsystem is achieved. The second part of the methodology, i.e. the contact economizer system, focuses on the recovery of low potential heat to further increase the efficiency of the system as discussed in section 3.3.

3.2 Pinch analysis

Basis of the method

The basis of this method was the amount of energy available within the IGCC system which could increase the overall performance of the system if utilized. The idea behind using pinch analysis, discussed in section 2.1 of Chapter 2, was to determine the maximum amount of steam ($\dot{m}_{steam}$) that could be generated from the excess heat or energy available ($Q_{available}$) within IGCC systems. This amount of steam would then be used to determine the corresponding power the steam turbine can generate, given its thermodynamic efficiency. The plant efficiency calculated using this power output of the steam turbine would then be the maximum possible for a given configuration of the plant. The following section gives a detailed discussion of the pinch analysis part of the methodology.

Method

Data of the plant is gathered using the first and most crucial step of pinch analysis, i.e. data extraction. The problem table algorithm steps are then applied to obtain the net heat flow at all shifted temperatures as discussed in section 2.2. The problem table results, i.e. the net heat flows and shifted temperatures, are then used to construct the Grand Composite Curve (GCC). From the GCC, the cold utility is determined and used to target the maximum steam flowrate ($\dot{m}_{steam}$) attainable under the given process constraints, i.e. the boiler and HRSG pressure. This targeting process can be divided into the following three stages:

- Stage 1 involves determining the amount of energy required to heat boiler feed water (BFW) with enthalpy H_{BFW} to saturated liquid with enthalpy H_{SL}. Saturation conditions in this case are determined by the boiler pressure. The BFW flowrate was assumed to be equal to the amount of steam generated, hence $\dot{m}_{steam}$ is also used to represent the flowrate of BFW.
- Stage 2 involves determining the amount of energy required to further heat the saturated liquid with enthalpy H_{SL} to saturated steam with enthalpy H_{SS} at the same boiler pressure.
- Stage 3 involves determining the amount of energy required to superheat the saturated steam leaving the boiler with enthalpy H_{SS} to superheated steam with enthalpy H_{SPS}, in the HRSG.

This three stage process can be represented by Equation (3.1) with $\dot{m}_{steam}$, the steam flowrate, being the only unknown.

$$Q_{avialable} = \dot{m}_{steam} \cdot (H_{SL} - H_{BFW}) + \dot{m}_{steam}\lambda_V + \dot{m}_{steam} \cdot (H_{SPS} - H_{SS}) \qquad (3.1)$$

λ_V represents the latent heat of vaporization of water for stage 2. From Equation (3.1), $\dot{m}$ can be calculated and used in Equation (3.2) to determine the energy carried by the superheated steam (Q_{SPS}). This energy is then used in

Equation (3.3) to determine the corresponding power output of the steam turbine ($\dot{W}_{ST}$).

$$Q_{SPS} = \dot{m}H_{SPS} \tag{3.2}$$

$$\eta_{ST} = \frac{\dot{W}_{ST}}{Q_{SPS}} \tag{3.3}$$

With the thermodynamic efficiency of the steam turbine (η_{ST}) known (set at 36% for this study), the power output of the steam turbine ($\dot{W}_{ST}$) is calculated and used in conjunction with the gas turbine power output ($\dot{W}_{GT}$) to calculate the gross IGCC efficiency (η_{IGCC}) as shown in Equation (3.4).

$$\eta_{IGCC} = \frac{\dot{W}_{ST} + \dot{W}_{GT}}{\dot{m}_{COAL} \cdot LHV_{COAL}} = \frac{\dot{W}_{ST} + \dot{W}_{GT}}{Q_{COAL}} \tag{3.4}$$

$\dot{m}_{COAL}$ represents the feed rate of coal while LHV_{COAL} and Q_{COAL}represent the low heating value and the calorific value of coal respectively. A heat exchange network design software, SuperTarget 6.0, is then used to create a heat exchange network from which a new process flowsheet can be constructed.

3.3 The contact economizer system

Basis of the method

Equation (3.1) leads to the basis of this method. Manipulation of this equation by replacing λ_V by $(H_{ss} - H_{sl})$ as per definition yields Equation (3.5).

$$Q_{available} = \dot{m}H_{sps} - \dot{m}H_{BFW} \tag{3.5}$$

The rearrangement of Equation (3.5) by simply writing $\dot{m}H_{sps}$ as the subject of the formula yields Equation (3.6), the overall energy balance of the plant. Equation (3.6) states that the energy carried by the superheated steam to the steam turbine (Q_{sps}) is equal to the sum of the energy available within the IGCC system ($Q_{available}$) and the energy enthalpy of the boiler feed water carried into the system.

$$\dot{m}H_{sps} = Q_{sps} = Q_{available} + \dot{m}H_{BFW} \tag{3.6}$$

If we consider or assume that $Q_{available}$ is constant, it is clear from Equation (3.6) that an increase in H_{BFW} will result in an increase in Q_{sps}. According to Equation (3.7), an increase in Q_{sps} results in an increase in $\dot{W}_{ST}$, which inturn, results in an increase in the gross thermal efficiency (η_{IGCC}) of the IGCC according to Equation (3.8).

$$\dot{W}_{ST} = \eta_{ST} Q_{sps} \tag{3.7}$$

$$\eta_{IGCC} = \frac{\dot{W}_{GT} + \dot{W}_{ST}}{Q_{coal}} \tag{3.8}$$

Substituting Equation (3.6) and Equation (3.8) into Equation (3.7), results into Equation (3.9), i.e. the basis of this method.

$$\eta_{IGCC} = \frac{\dot{m}\eta_{ST}}{Q_{coal}}(H_{BFW}) + \frac{\dot{W}_{GT} + \eta_{ST}.Q_{available}}{Q_{coal}} \tag{3.9}$$

If we consider keeping $\dot{m}$ constant, for example in the case where a maximum $\dot{m}$ possible to satisfy the cooling was obtained, Equation (3.9) is then a straight line equation where η_{IGCC} is only function of H_{BFW}. It is evident from Equation (3.9) that an increase in H_{BFW} will result in an increase in η_{IGCC}. This important observation led to the contact economizer system method discussed in the following section.

Method

The contact economizer system method developed is divided into 2 parts, i.e. determining the maximum boiler feed water temperature attainable and applying Mickley's graphical technique for dehumidification to demonstrate how the aforementioned temperature is achieved. The Grand Composite Curve is used to check whether the determined boiler feed water temperature is feasible.

Application of this method with reference to Figure 3.1 is as follows:

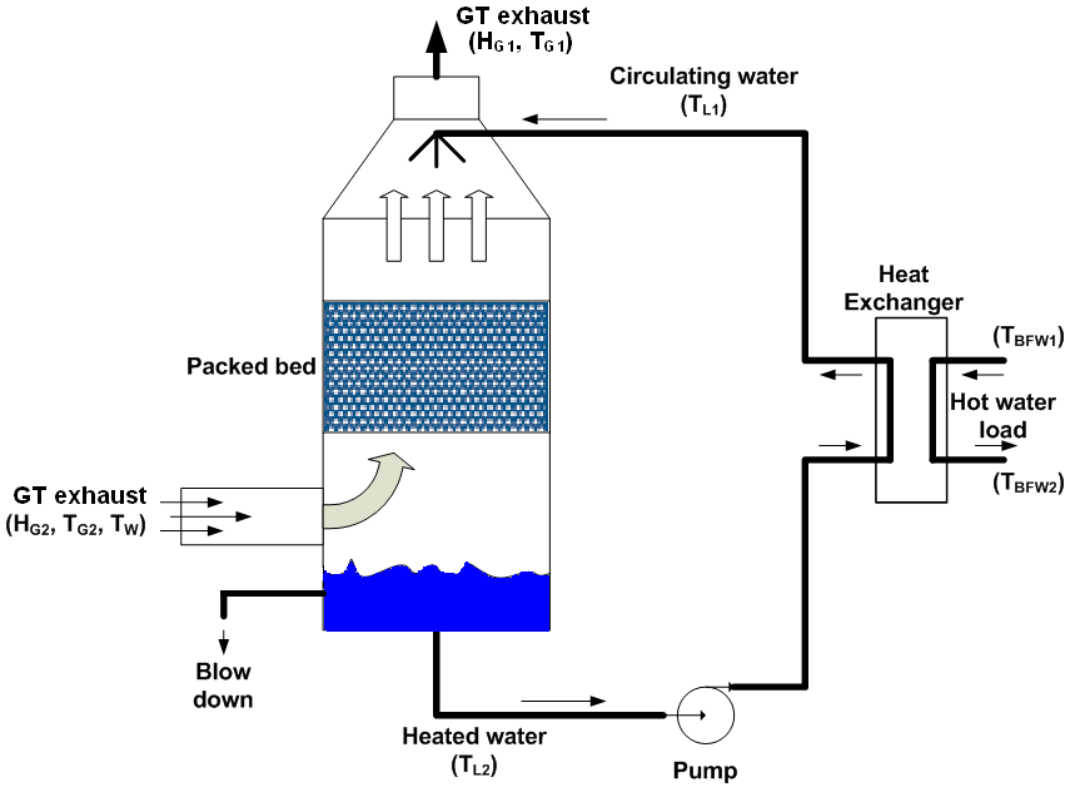

Figure 3.1: Necessary stream data for the application of the contact economizer system

Given the conditions of the GT exhaust ($G, H_{G2}, T_{G2}\ and\ T_w$):

Part 1: detemining the maximum BFW temperature.

1. Specify a "$\Delta T_{\min\ \_column}$" for the packed column and a "$\Delta T_{\min\ \_HX}$" for the heat exchanger.
2. Specify T_{L2} to be at least "$\Delta T_{\min\ \_column}$" lower than the wet-bulb temperature (T_w) of the gas to allow for thermal driving forces.
3. Determine the maximum attainable T_{BFW2} that does not violate "$\Delta T_{\min\ \_HX}$" in the heat exchanger then calculate the corresponding η_{IGCC} from Equation (3.6). Validation of T_{BFW2} is done on the Grand Composite Curve.

Part 2: applying Mickley's graphical technique for dehumidification.

4. Draw the equilibrium curve on the "H_G" vs. "T_L" graph.
5. Specify the circulating water flowrate (L) then calculate the L/G ratio.
6. Draw the operating line using Equation ($2.12c$) and apply Mickley's graphical technique to determine the gas dehumidification path as follows:
   - 6.1 Specify T_{G1} and H_{G1} such that the gas is still above its condensation point.
   - 6.2 Choose a starting $-h_L a_H / k_G a_M$ and apply Mickley's graphical technique to determine the dehumidification path.
   - 6.3 Check if the dehumidification path intersects the point $(T_G, H_G) = (T_{G1}, H_{G1})$ in step 6.1 and proceed as follows:
     - If the dehumidification path intersects the point

$(T_G, H_G) = (T_{G1}, H_{G1})$, then the design can be carried out with the specified $-h_L a_H / k_G a_M$ ratio.

- Otherwise repeat steps 6.2 and 6.3 while changing $-h_L a_H / k_G a_M$ in step 6.2 until the dehumidification path intersects the aforementioned point.

7. Repeat steps 5 and 6 with a new L/G ratio to optimize the cooling process.
8. Determine the tower height (Z) as discussed below.

Determining the tower height after obtaining the $-h_L a_H / k_G a_M$ ratio becomes a matter of solving three simple simultaneous equations. The integrals in the left hand side of Equations $(2.6b)$ and $(2.13b)$ can be solved graphically after determining the dehumidification path. In addition to the determined $-h_L a_H / k_G a_M$ ratio, this leaves us with three equations and three unknowns of which the tower height (Z) is one of them. The other two unknowns are $h_L a_H$ and $k_G a_M$. The three equations can then be solved for these three unknowns, hence determining the exact transfer (heat and mass) coefficients required for the process.

3.4 Conclusion

This Chapter gives a detailed discussion of the proposed methodology to increase the efficiency of IGCC plants. The proposed methodology is divided into 2 parts, i.e. pinch analysis for efficient utilization of energy within the plant and the contact

economizer system for recovery of low potential heat. The pinch analysis part of the methodology, as discussed in section 3.2, focuses on improving the structure of the steam-path subsystem such that the utilization of energy within the plant is maximized. The contact economizer system part of the methodology, on the other hand, is divided into 2 parts, i.e. determining the maximum BFW temperature attainable and applying Mickley's graphical technique for dehumidification, following a slightly different procedure that allows for calculation of the exact ratio between the liquid-phase heat transfer coefficient and the gas-phase mass transfer coefficient, to demonstrate how the aforementioned BFW temperature is achieved. Section 3.3 demonstrated that a higher BFW temperature improves the performance of the plant, hence the contact economizer system method.

4. APPLICATION OF METHODOLOGY

4.1 Introduction

This chapter discusses the application of the methodology developed in chapter 3. Application of the two parts of the methodology, i.e. pinch analysis and the contact economizer system, is discussed separately. A brief discussion on the case study is given prior to the application of the methodology.

4.2 Case study

The world's largest capacity IGCC, i.e. the Elcogas power plant, was used as a case study in this thesis. Figure 4.1 is the process flow sheet of the Elcogas power plant.

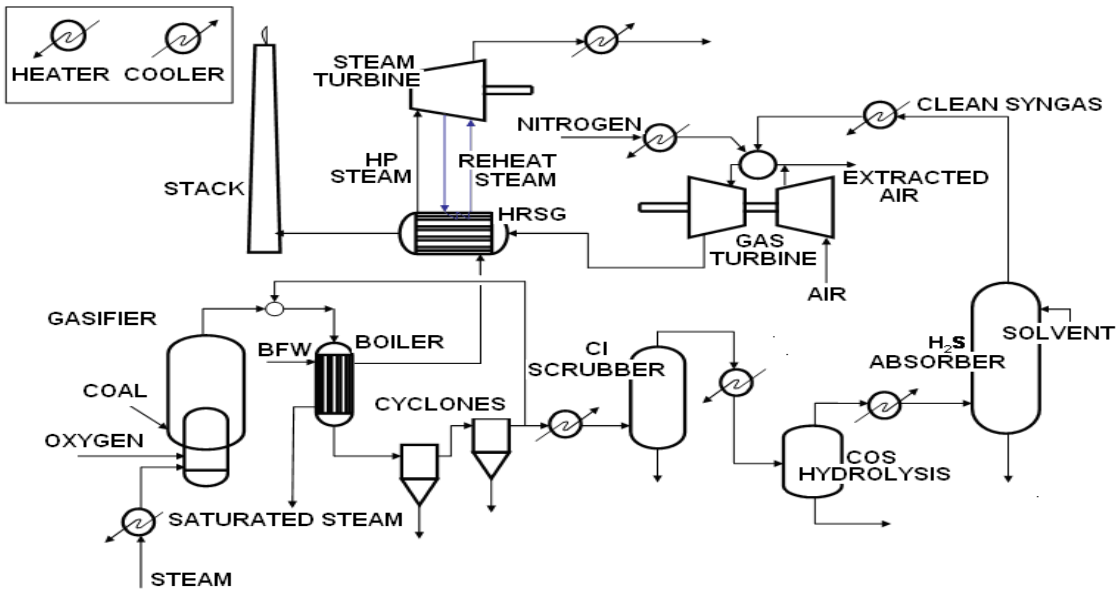

Figure 4.1: Simplified flowsheet of the Elcogas plant

The process followed by this plant is similar to the process discussed in section 1.2. The gas path starts from the gasifier exit stream, goes through the boiler and cleaning section (cyclones, Cl srubber, COS hydrolysis and H_2S absorber), then through the gas turbine and ends up in the stack. The steam path on the other hand starts at the boiler as boiler feed water (BFW), goes through the HRSG then finally through the steam turbine. Both the boiler and the HRSG are at a pressure of 127 bar (Thermie programme, 2000). The mass flowrate of steam responsible for power generation in the steam turbine of this plant is 85.6 kg/s. This plant has a net capacity of 335 MW and a gross efficiency of 47% (Elcogas, 2005). The power output of the gas turbine ($\dot{W}_{GT}$) is 200 MW while the steam turbine power output ($\dot{W}_{ST}$) is 135 MW.

4.3 Application of pinch analysis

Figure 4.2 shows the process streams that were extracted from the plant for pinch analysis. The red and blue lines in Figure 4.2 represent the hot and the cold streams respectively. The corresponding supply temperatures (T_{supply}) and target (T_{target}) temperatures for the streams are given in Table 4.1 along with the enthalpy/energy (ΔH) carried or required by the streams. Table 4.2 shows a detailed problem table for the process. The shifted temperatures (T^*) are indicated in the first column of Table 4.2 while the net heat flow cascade (ΔH cascade) is indicated in the last column of Table 4.2. ΔH is the enthalpy at any temperature interval (i) calculated from Equation (2.1). No hot utility was required in this process since the first ΔH cascade value was zero. The amount of cold utility Table 4.2 shows a detailed problem table for the process. The shifted temperatures (T^*) are indicated in the first column of Table 4.2 while the net heat flow cascade (ΔH cascade) is indicated in the last column of Table

4.2. ΔH is the enthalpy at any temperature interval (i) calculated from Equation (2.1).

No hot utility was required in this process since the first ΔH cascade value was zero.

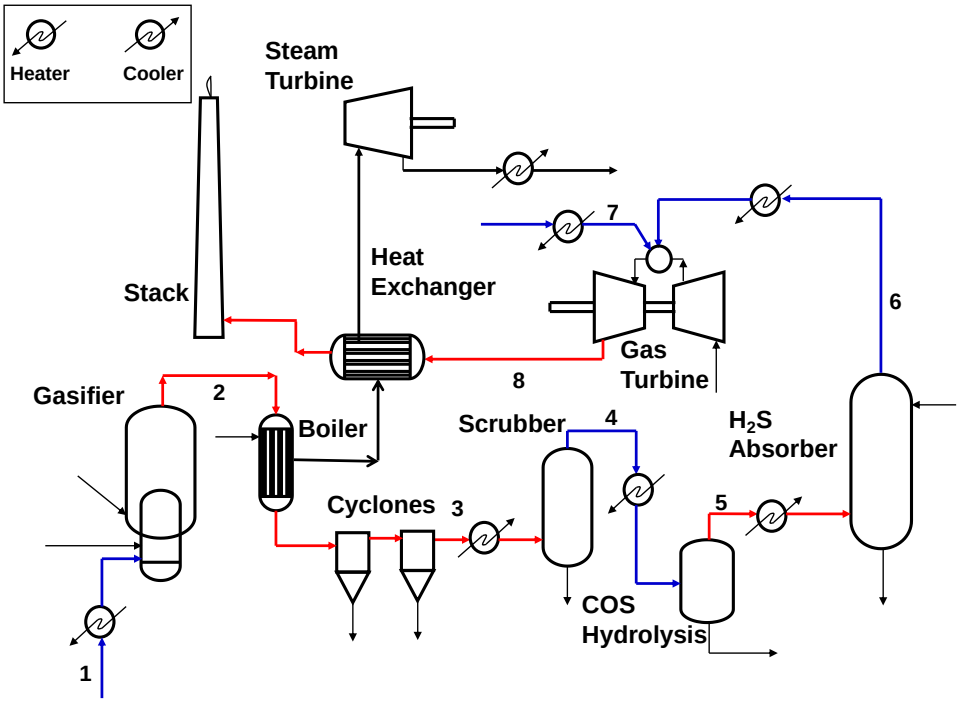

Figure 4.2: Streams extracted from the process for pinch analysis

Table 4.1: Stream data

Stream No.	Stream name	Stream type	T_{supply} (°C)	T_{target} (°C)	ΔH (MW)
1	Steam_Gen	Cold	25	240	42.4
2	Raw_Syngas	Hot	800	235	45.8
3	Particulate_Free	Hot	235	35	12
4	COS_Rich	Cold	35	130	5
5	COS_Free	Hot	140	35	20
6	Sweet_Syngas	Cold	35	350	17
7	Nitrogen	Cold	180	480	21
8	GT_Exhaust	Hot	650	90	442.4

The amount of cold utility required/energy available was 434.8 MW as indicated by the last ΔH cascade value in Table 4.2.

Table 4.2: The problem table for the case study

T* (°C)	Temperature interval (i)	ΔT* (°C)	Streams in temperature interval (i)	$\sum CP_H - \sum CP_C$ (MW/°C)	ΔH (MW)	ΔH cascade (MW)
800						**0**
	1	150	2	0.081	12.16	
650						12.16
	2	160	2,8	0.871	139.37	
490						151.53
	3	130	2,8,7	0.801	104.14	
360						255.67
	4	110	2,8,7,6	0.747	82.18	
250						337.85
	5	15	2,8,7,6,1	0.550	8.25	
235						346.10
	6	45	8,7,6,1,3	0.529	23.80	
190						369.89
	7	50	8,6,1,3	0.599	29.94	
140						399.83
	8	0	8,6,1,3,4	0.546	0.00	
140						399.83
	9	50	8,6,1,3,4,5	0.737	36.83	
90						436.67
	10	45	6,1,3,4,5	-0.053	-2.40	
45						434.27
	11	10	1,3,5	0.053	0.53	
35						**434.80**

Figure 4.3 shows the grand composite curve (GCC) constructed using T^* and ΔH cascade in Table 4.2. The three stage process for generating the maximum mass flowrate of steam, as discussed in section 3.1, is also shown in Figure 4.3. In stage 1, BFW at 25ºC and boiler pressure of 127 bar was heated to a saturation temperature of 329 ºC. The change in enthalpy for stage 1 was 1403 kJ/kg. The latent heat of vaporization (λ_V) of stage 2 at 329 ºC and the aforementioned boiler pressure was 1150 kJ/kg. Stage 3 on the other hand had a change in enthalpy of 688 kJ/kg, resulting in the superheated steam leaving the HRSG at a temperature of 506 ºC.

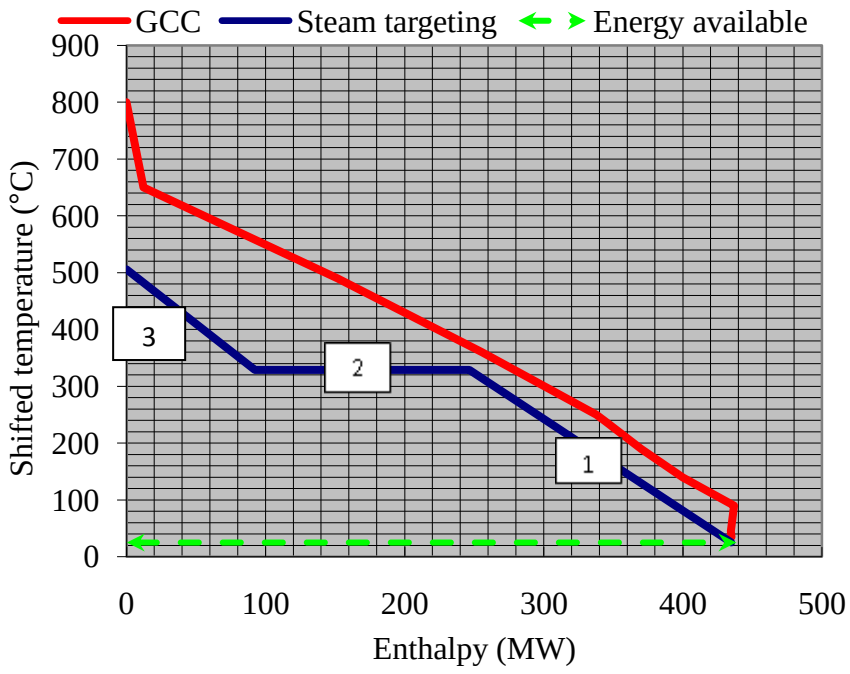

Figure 4.3: The grand composite curve

With the change in enthalpies for the three phases and the energy available ($Q_{available}$) known, a maximum mass flow rate of 134 kg/s of steam was calculated from Equation (3.1). The rest of the values calculated are given below:

- $\dot{W}_{ST} = 162\ MW$
- $\eta_{IGCC} = 0.54$

The new process flowsheet designed to satisfy the values calculated above is shown in Figure 4.4. The dashed line in Figure 4.4 represents the new steam-path. It is worth mentioning that the supply temperatures (T_{supply}) and the target temperatures (T_{target}), to and from the units, remain unchanged from the preliminary design.

4.4 Application of the contact economizer system

Application of the contact economizer system (CES) was on the gas turbine exhaust stream of the design shown in Figure 4.4 which enters the stack at a temperature of 90°C. The composition of this gas turbine exhaust stream was assumed to be the design composition of a typical IGCC plant and the rest of the design data is given in Table 4.3. The exhaust gas was assumed to behave like air under these conditions. Consequently, enthalpy data was obtained from the air-water psychometric chart. The 8 step methodology given in section 3.2 was followed in the application of the CES to increase η_{IGCC}.

Table 4.3: Data for the heat integrated design

Property	Magnitude
$\dot{m}$	134.2 kg/s
η_{ST}	0.36
η_{IGCC}	0.54
$\dot{W}_{GT}$	200 MW
$Q_{available}$	434.8 MW
Q_{coal}	669.3 MW

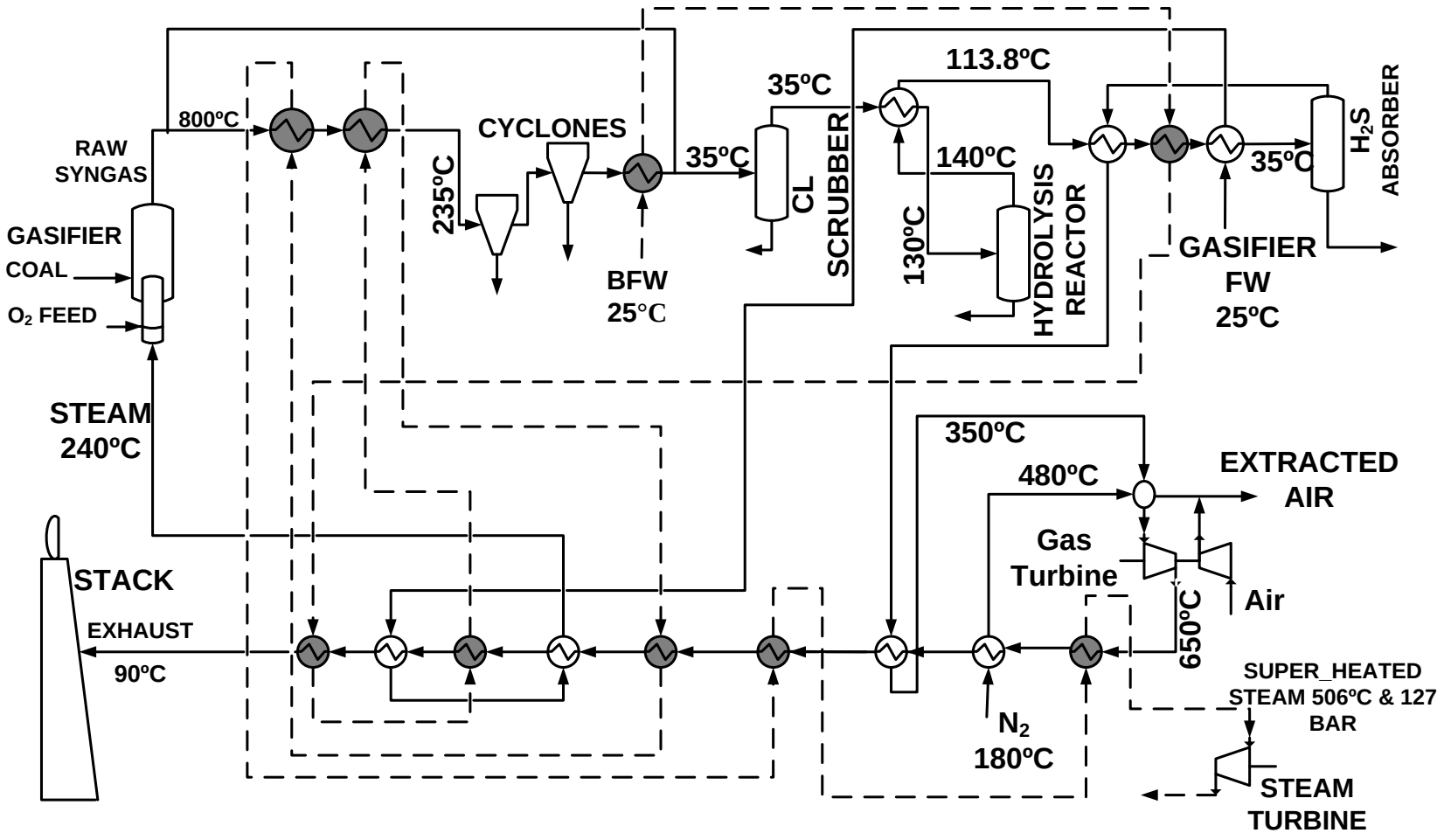

Figure 4.4: Energy optimized design of the Elcogas plant

Figure 4.5 shows the results of the case study after application of the 8 step graphical methodology. These results were obtained at an L/G ratio of 1.1. The maximum attainable T_{BFW2} was found to be 57.3°C.

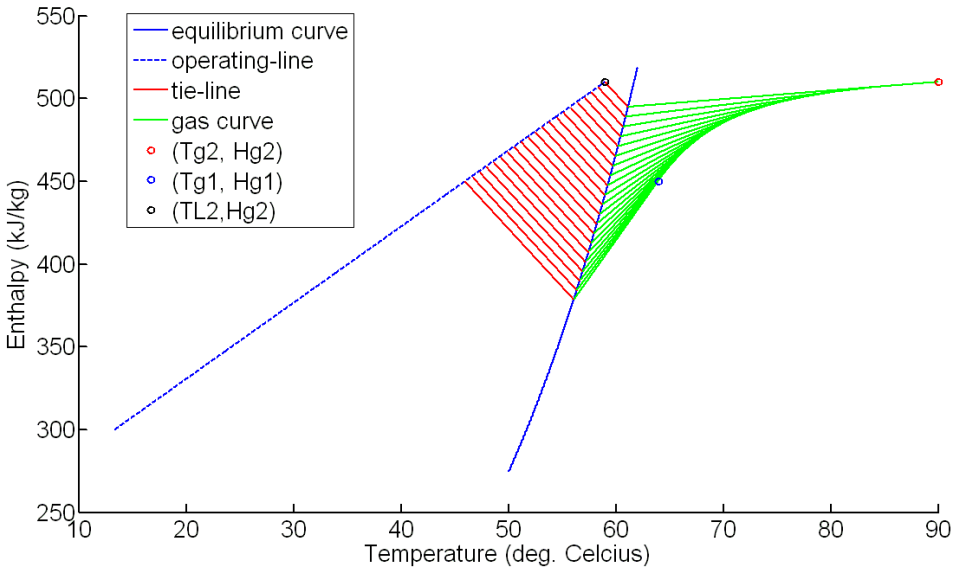

Figure 4.5: Results of Mickley's graphical technique at an L/G ratio of 1.1

Figure 4.6 shows the GCC of the process discussed in the case study with a new steam target. The dashed yellow line in Figure 4.6 represents the effect of increasing the BFW temperature to the aforementioned T_{BFW2} value, on the system. In other words, the dashed yellow line represents the new steam target after increasing the inlet BFW temperature to T_{BFW2}.

It is evident from the first slope of the dashed yellow line, which is the same as the first slope of the initial steam target represented by the blue solid line, that the heat capacity flowrate (*CP*) is kept constant. Since *CP* is given by the product of specific heat capacity and BFW flowrate ($\dot{m_{steam}}$), it follows that at a constant ($\dot{m_{steam}}$), the

specific heat capacity also remains constant to maintain the same *CP* used in the initial steam targeting.

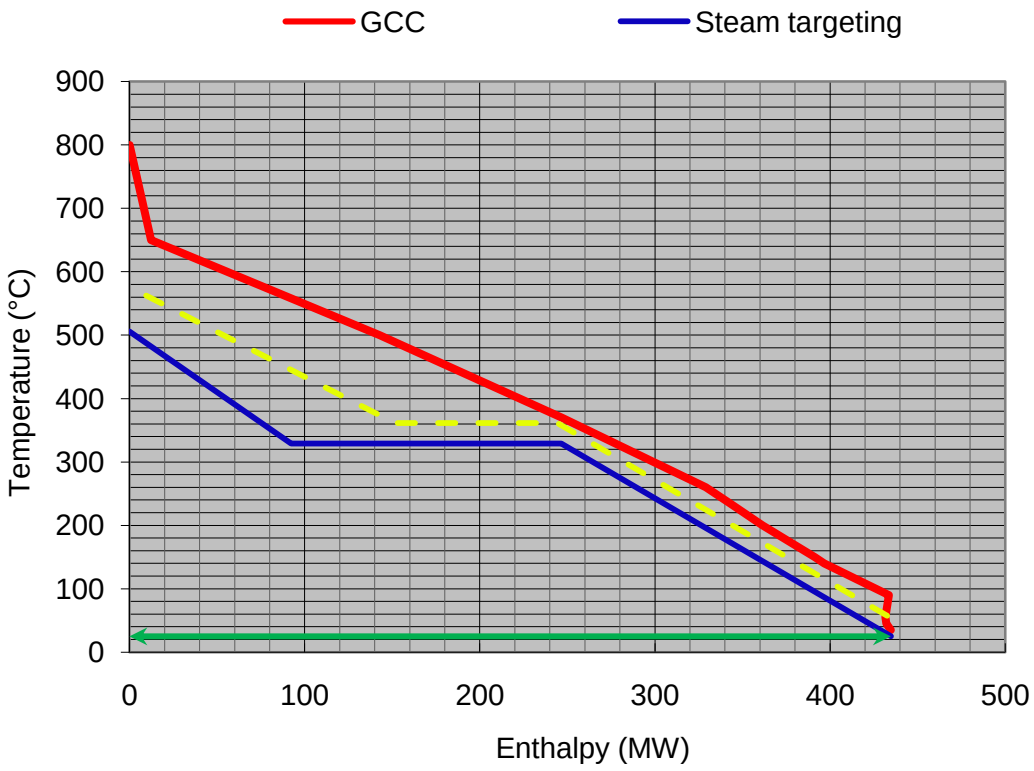

Figure 4.6: The Grand Compostie Curve with a new steam target

Consequently, for a higher BFW temperature, i.e. the aforementioned T_{BFW2}, a higher boiler pressure is required to maintain the same *CP*. In this case, a boiler and HRSG pressure of 189 bar was required as opposed to the initial boiler pressure 120 bar for initial steam target. This resulted in an increase in η_{IGCC} from 0.54 to 0.55. A T_{L2} of 59°C at a $\Delta T_{\min\ \_column}$ of 3°C satisfied the required conditions for step 3 of the of the aforementioned methodology, while a $\Delta T_{\min\ \_HX}$ of 1.7°C was maintained for the heat exchanger. The outlet gas temperature and enthalpy ($T_{G1}\ and\ H_{G1}$) where specified to be 64°C and 450kJ/kg as indicated by the small blue circle on the gas curve of Figure 4.5.

The corresponding $-h_L a/k_G a$ that satisfied the conditions of step 5 of the methodology was 7.04 kJ/kgK. Further improvements could be done to these results to improve the cooling process by altering L/G as explained in step 7 of the methodology. Figure 4.7 shows the results of Mickley's graphical technique at an L/G ratio of 1.5 and the same $-h_L a/k_G a$ ratio used in constructing Figure 4.5.

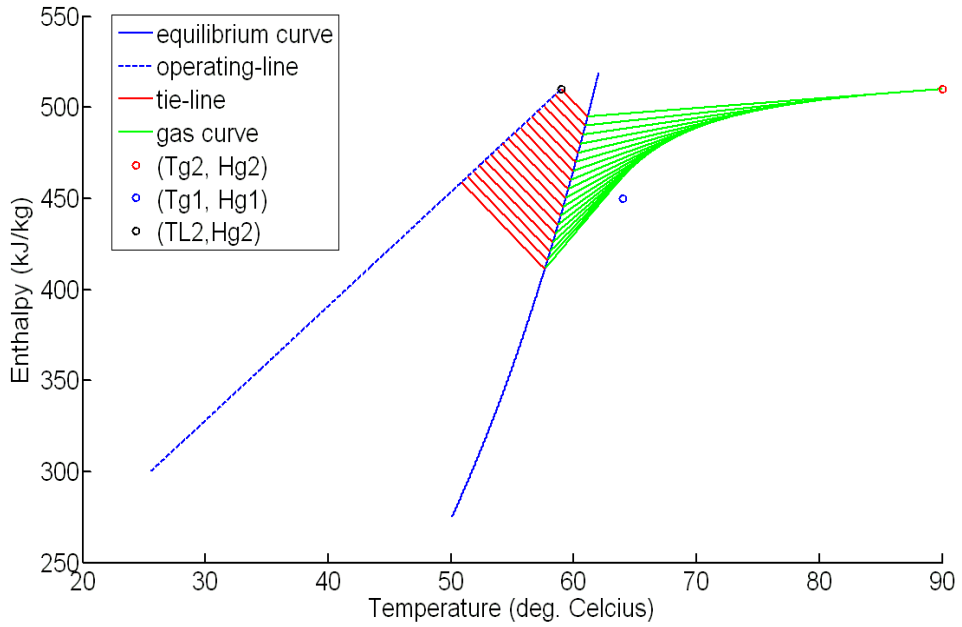

Figure 4.7 : Results of Mickley's graphical technique at an L/G ratio of 1.5

It is evident from Figure 4.7 that temperature driving forces, i.e. the space between the gas curve and the equilibrium curve, are larger at the bottom of the column and decrease rapidly as the gas approaches outlet conditions (T_{G1}, H_{G1}) at the top of the column. Infact, cooling is so rapid at the bottom of the column in such a way that the gas does not meet the outlet conditions, i.e. the gas curve does not intersect the point (T_{G1}, H_{G1}). In order to meet the outlet conditions at a higher L/G ratio, a larger

$-h_L a/k_G a$ ratio is required. For the case considered in Figure 4.7, an $-h_L a/k_G a$ ratio of 8.992 kJ/kgK meets the gas outlet conditions as shown in Figure 4.8.

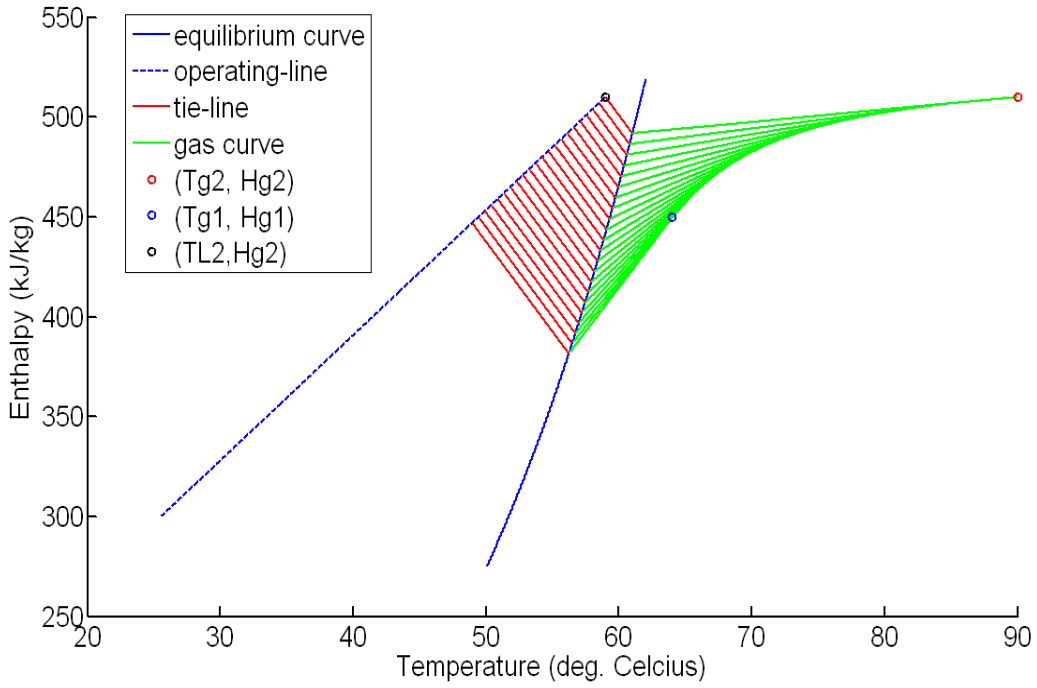

Figure 4.8: Results of Mickley's graphical technique at an L/G ratio of 1.5

Figure 4.9 shows the results of Mickley's graphical technique at an L/G ratio of 0.8 and the same $-h_L a/k_G a$ ratio used in constructing Figure 4.5. It is evident from Figure 4.9 that temperature driving forces decrease gradually as the gas approaches outlet conditions (T_{G1}, H_{G1}) at the top of the column. In this case, the outlet gas exits at a temperature higher than the specified temperature (T_{G1}). In order to meet the outlet conditions at a lower L/G ratio, a smaller $-h_L a/k_G a$ ratio is required. For the case considered in Figure 4.9, an $-h_L a/k_G a$ ratio of 5.761 kJ/kgK meets the gas outlet conditions as shown in Figure 4.10.

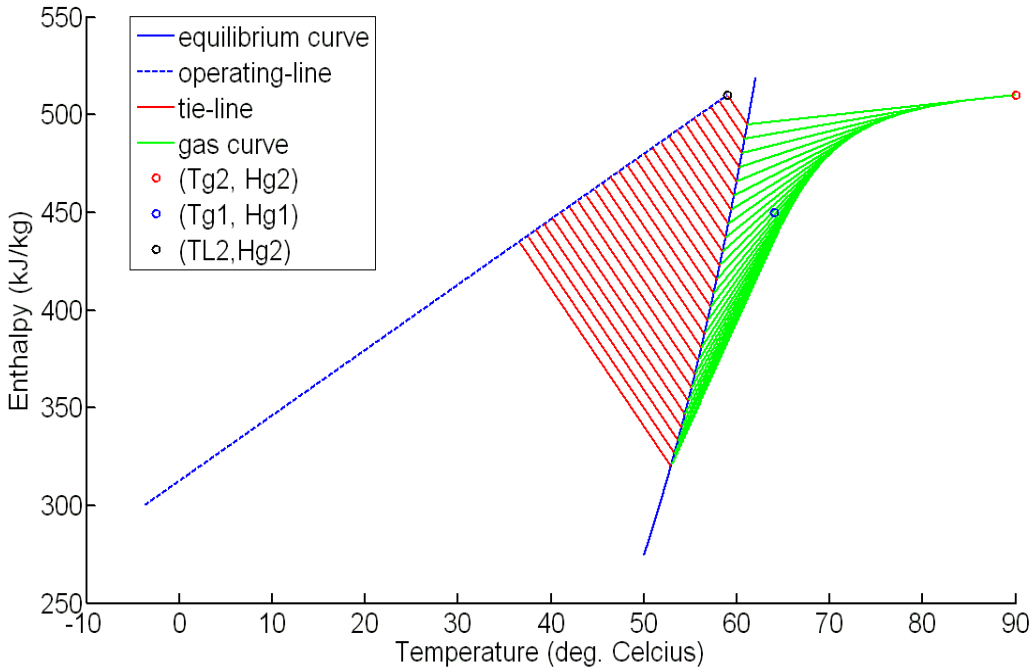

Figure 4.9: Mickley's graphical technique at an L/G ratio of 0.8.

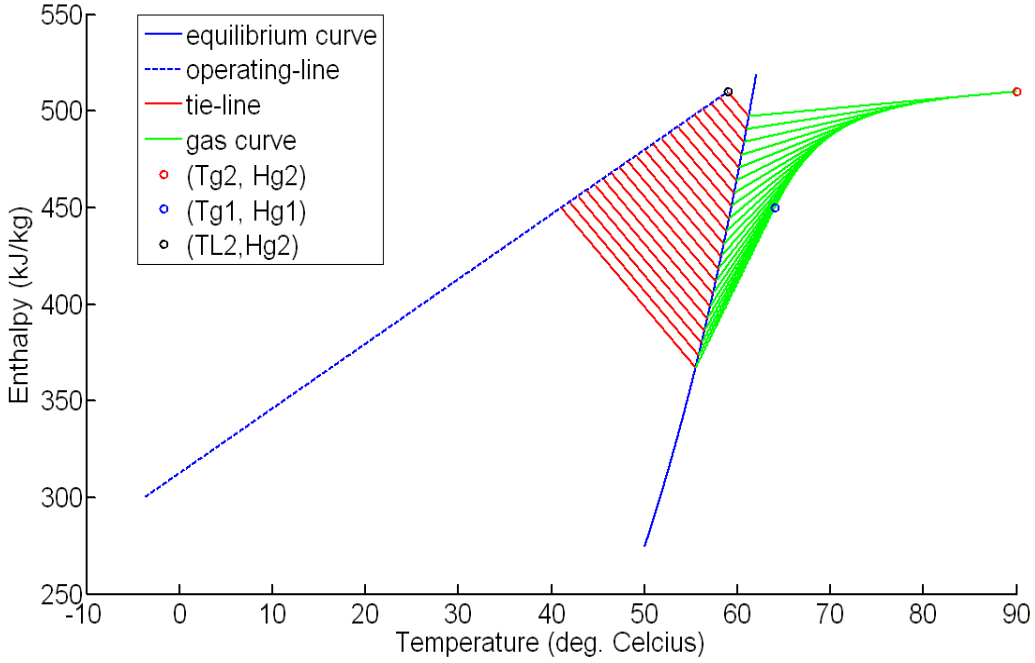

Figure 4.10: Mickley's graphical technique at an L/G ratio of 0.8

This optimization of the cooling/dehumidification process is entirely influenced by the design requirements of the tower hence it was not included in this thesis, but rather the application of the proposed methodology is emphasized.

5. CONCLUSION

The IGCC system has proved to be superior to conventional coal power generation plants in its few years of operation. Studies on further improving the performance of the IGCC system are currently at an advanced stage. The development of new technology and the experience gained in the past years of operation have brought insights on ways to improve the performance of the IGCC system. A lot work proposed so far, however, is still facing challenges that are hindering its application. It is, however, a matter of time before the ultimate goal of using IGCC system is achieved, i.e. achieving very high efficiencies at near zero, if not zero, emission levels.

An energy optimization method to optimize the use of energy available within the IGCC system was presented. This method is divided into two parts, i.e. pinch analysis for targeting the maximum flowrate of steam and designing an optimized heat exchanger network, and the contact economizer system for low potential heat recovery. A case study on the Elcogas plant illustrated that the developed method is capable of increasing the gross efficiency from 47% to 55%. This increase in efficiency, however, comes at an expense of increased heat exchange area required to exchange the extra heat that was not utilized in the preliminary design.

A lot of improvement on IGCC systems can still be done. None of the studies so far have considered combining the three optimization methods mentioned in section 2.6, i.e. gas path optimization and integration, steam path optimization and energy

optimization. It is only logical to assume that the ultimate efficiency of IGCC systems can only be achieved if both paths and the energy within the system are optimized.

References

Bayarsaikhan, B, Sonoyama, N, Hosokai, S, Shimada, T, Hayashi, JI and Li, CZ (2006), "Inhibition of steam gasification of char by volatiles in a fluidized bed under continuous feeding of a brown coal," *Fuel*, 85, 340–349.

Bi, XT, & Liu, X (2010), "High density and high solids flux CFB risers for steam gasification of solids fuels," *Fuel Processing Technology*, 91, 915– 920.

Corella, J, Toledo, JM, and Molina, G (2007), "A review on dual fluidized-bed biomass gasifier," *Industrial & Engineering Chemistry Research*, 46, 6831–6839.

Elcogas (2005), "Operating experience and current status of Puertellano IGCC power plant," International Freiberg Conference on IGCC & Xtl Technologies, http://www.elcogas.com/elcogas_en/

Emun, F, Gadalla, M, Majozi, T and Boer, D (2010), "Integrated gasification combined cycle (IGCC) process simulation and optimization" *Computers and Chemical Engineering*, 34, 331-334.

Geosits, RS and Lee, AS (2005), "IGCC – The challenges of integration," Proceeding for GT2005, Bechtel Corporation, Houston.

Giuffrida, A, Romano, MC and Lozza, GG (2010), "Thermodynamic assessment of IGCC power plants with hot fuel gas desulfurization," *Applied Energy*, 87, 3374-3383.

Guan, G, Fushimi, C, Tsutsumi, A, Ishizuka, A and Matsuda, M (2010), "High-density circulating fluidized bed gasifier for advanced IGCC/IGFC – Advantages and challenges," *Particuology*, 230, 1-5.

Hayashi, JI, Hosokai, S, and Sonoyama, N (2006), "Gasification of low-rank solid fuels with thermo chemical energy recuperation for hydrogen production and power generation," *Process Safety and Environmental Protection*, 84(6), 409–419.

Jiang, L, Lin, R, Lin, H, Cai, R and Liu, Z (2002) "Study on thermodynamic characteristic and optimization of steam cycle system in IGCC" *Energy Conversion and Management*, 43, 1339-1348.

Kemp, IC (2007), *Pinch Analysis and Process Integration*, 2nd edition, Elsevier, London.

Kim, YS, Lee, JJ, Kim, TS, Sohn, JL and Joo, YL (2010), "Performance analysis of syngas-fed gas turbine considering the operating limitations of its components," *Applied Energy*, 87, 1602-1611.

Kuchonthara, P, Battacharya, S, and Tsutsumi, A (2005), "Combination of thermo-chemical recuperative coal gasification cycle and fuel cell for power generation," *Fuel*, 84, 1019–1021.

Lee, JJ, Kim, YS, Cha KS, Kim TS, Sohn, JL and Joo, YJ (2009), "Influence of system integration options on the performance of an integrated gasification combined cycle power plant," *Applied Energy*, 86, 1788-1796.

Linnhoff, B and Flower, JR (1978), "Synthesis of heat exchanger networks, I. Systematic generation of optimal networks," *AICHE*, 24 (4), 633- 642.

Lou, Y, Smith, R and Sadhukhan, J (2008), "Decarbonisation in Energy Production," Centre for Process Integration, Chemical Engineering & Analytical Science, The University of Manchester, Manchester, United Kingdom.

Mickley HS, (1949), "DESIGN OF FORCED DRAFT AIR CONDITIONING EQUIPMENT," *Chem. Engng. Prog.*, 45, 739-749.

Minchener, AJ (2005), "Coal gasification for advanced power generation," *Fuel*, 84, 2222-2235.

Ohtsuka, Y, Tsubouchi, N, Kikuchi, T, Hashimoto, H (2009), "Recent progress in Japan on hot gas cleanup of hydrogen chloride, hydrogen sulfide and ammonia in coal derived fuel gas," *Powder Technol*, 190, 340–347.

Profiles (2006), "Coal gasification and IGCC in Europe," http://www.iea-coal.org.uk/publishor/system/component_view.asp?LogDocId=81458.

Shilling, NZ and Lee, DT (2003), "IGCC-Clean power generation alternative for solid fuels," *PowerGen Asia*.

Smith, R (2005), *Chemical Process Design and Integration*, 2nd edition, John Wiley & Sons.

The Energy Blog (2005), "About the IGCC Power Plants," http://www.thefraserdomain.typepad.com/energy/2005/09/about_igcc_powe.html.

The International Energy Agency (IEA) Green Gas R&D Programme (2007), "Capturing CO_2," www.**iea**ghg.org/docs/general_publications/co**capture**.pdf.

Thermie programme (2000), "IGCC Puertollano: A clean coal gasification power plant," http://212.170.221.11/elcogas_body/images/IMAGEN/TECNOLOGIAGICC/thermie.pdf

US DoE (2000) "Tampa Electric Integrated Gasification Combined Cycle Project: An Update", Tropical Report number 19, Department of Energy, United States.
Vamvuka, D, Arvanitidis, C and Zachariadis D (2004), "Flue gas desulfurization at high temperatures: a review," *Environ Eng Sci*, 21, 525–547.

Venkataraman C, (2009), "Cooling Tower- MT 305" CL 332/334- UG LAB, http://www.che.iitb.ac.in/courses/uglab/manuals/coollabmanual.pdf.

Vlaswinkel, EE (1992) "Energetic analysis and optimisation of an integrated coal gasification-combined cycle power plant" *Fuel Processing Technology*, 32 (1992), 47- 67.

Yong, KH (2007), "Method of gasification in IGCC system," *International Journal of Hydrogen Energy*, 34, 5088-5093.

Zhelev TK, and Semkov KA, (2004), "Cleaner flue gas and energy recovery through pinch analysis," *Journal of Cleaner Production*, 12, 165-170.

Zheng, L and Furinsky, E (2005), "Comparison of Shell, Texaco, BGL and KRW gasifiers as part of IGCC plant computer simulations," *Energy Conversion and Management*, 46, 1767 – 1779.